

# 000 001 002 003 004 005 006 007 008 009 010 011 012 013 014 015 016 017 018 019 020 021 022 023 024 025 026 027 028 029 030 031 032 033 034 035 036 037 038 039 040 041 042 043 044 045 046 047 048 049 050 051 052 053 REMAINING-DATA-FREE MACHINE UNLEARNING BY SUPPRESSING SAMPLE CONTRIBUTION

Anonymous authors

Paper under double-blind review

## ABSTRACT

Machine unlearning (MU) aims to remove the influence of specific training samples from a well-trained model, a task of growing importance due to the “right to be forgotten.” The unlearned model should approach the retrained model, where forgetting data do not contribute to the training process. Therefore, unlearning should withdraw their contribution from the pre-trained model. However, quantifying and disentangling sample’s contribution to overall learning process is highly challenging, leading most existing MU approaches to adopt other heuristic strategies such as random labeling or knowledge distillation. These operations inevitably degrade model utility, requiring additional maintenance with remaining data. To advance MU towards better utility and efficiency for practical deployment, we seek to approximate sample contribution with only the pre-trained model. We theoretically and empirically reveal that sample’s contribution during training manifests in the learned model’s increased sensitivity to it. In light of this, we propose MU-Mis (Machine Unlearning by Minimizing input sensitivity), which directly suppresses the contribution of forgetting data. This straightforward suppression enables MU-Mis to successfully unlearn without degrading model utility on the remaining data, thereby eliminating the need for access to the remaining data. To the best of our knowledge, this is the first time that a remaining-data-free method can [perform on par with top performing remaining-data-dependent methods](#).

## 1 INTRODUCTION

Deep neural networks (DNNs) are revealed to store information of training data (Feldman, 2020; Feldman & Zhang, 2020; Tian et al., 2025) and such information could be reproduced by privacy attacks (Shokri et al., 2017; Zhu et al., 2019), raising data privacy concerns. The “right to be forgotten” (Regulation, 2018) is introduced to safeguard user privacy, which entails ensuring that the DNN performs as if the data were never involved in the training.

While retraining from scratch would ideally achieve this, it is often infeasible due to the high cost of training DNNs. This has motivated the study of “*Machine Unlearning*” (MU) (Cao & Yang, 2015), which fine-tunes the *pre-trained model* to approach the *retrained model* as closely as possible. The essential distinction in pre-trained and retrained model lies in the contribution of forgetting data, whose role shift from “contributors” that affect parameter updates in the pre-trained model to “bystanders” that exert no influence in the retrained model. Therefore, unlearning should aim to withdraw their contribution to the learning process.

However, identifying such a contribution is highly challenging. Learning is a dynamic process that gradually remembers and assimilates data, while unlearning, which is the reverse process that gradually removes data information, is achieved by backtracking the training trajectory to withdraw historical gradients in early study (Graves et al., 2021; Thudi et al., 2022). Nevertheless, such tracking not only contradicts the efficiency demands of unlearning but also yields limited effectiveness due to the incrementality of training (Wang et al., 2024b).

Consequently, most existing MU methods circumvent the difficulty of estimating sample contribution through other heuristics. A common strategy is to introduce confusion, *e.g.*, random relabeling (Golatkar et al., 2020; Graves et al., 2021; Fan et al., 2024b) or knowledge distillation from useless teacher (Chundawat et al., 2023; Kurmanji et al., 2023). However, these approaches suffer from

several limitations: (i) such confusion causes *catastrophe unlearning* (Wang et al., 2024b) or *over-forgetting* (He et al., 2025), i.e., severe degradation of model utility on the remaining data; (ii) the degradation in turn necessitates costly maintenance using the remaining data, thereby substantially *undermining MU efficiency*; (iii) the remaining data are not always accessible in practice. These limitations collectively underscore the importance of moving beyond heuristic confusion strategies and developing more principled unlearning mechanisms to advance MU toward higher utility and efficiency. Therefore, although quantifying sample contribution is inherently challenging, in this paper, we make efforts to ground unlearning in a precise characterization of sample’s contribution.

Instead of accumulating the historical contributed gradient update during training, we identify the clue of contribution directly from the derivative of the training algorithm w.r.t a training sample. The learning process is a mapping by the training algorithm  $\mathcal{A}$  from the training set  $\mathcal{D} = \{(x_i, y_i)\}$  to a learned function  $f$ : denoted as  $f = \mathcal{A}(\mathcal{D})$ . Therefore, the training sample  $x_i$  contributes to the output:  $\partial \mathcal{A} / \partial x_i \neq 0$  while a sample out of the training set does not. A simple yet enlightening example lies in the support vector machine (Cortes & Vapnik, 1995; Christmann & Steinwart, 2008), where only the training data can act as support vectors that impact the decision boundary. Thus, withdrawing the sample contribution can be achieved by suppressing  $\partial \mathcal{A} / \partial x_i$ .

The main challenge is that  $\mathcal{A}$  corresponds to a dynamic training process without a closed-form expression. To address this, we theoretically illustrate that  $\partial \mathcal{A} / \partial x_i$  could be approximated by the learned model’s sensitivity to its input  $x$ , i.e.  $\partial f(x) / \partial x$  with  $f = \mathcal{A}(\mathcal{D})$  in Section 3.2. To derive a principled and optimization-friendly guideline aligned with the behavior of a retrained model, we delve deeper into the input sensitivity across different logits. Our empirical investigations under the machine learning (Section 3.3) and machine unlearning (Section 3.4) scenarios reveal that a sample’s contribution manifests as disproportionately higher input sensitivity of the target logit relative to irrelevant logits. In light of this finding, we propose **MU-Mis** (Machine Unlearning by Minimizing Input Sensitivity), which suppresses sample contribution by reducing the sensitivity disparity between the target and non-target logits to the forgetting data.

We evaluate MU-Mis on 3 standard unlearning tasks across 6 datasets, benchmarking against 6 competitive remaining-data-dependent unlearning methods and 4 existing remaining-data-free baselines. The results demonstrate that MU-Mis achieves effective unlearning while preserving model utility on the remaining data **without utilizing them**, performing on par with SoTA remaining-data-dependent approaches and outperforming all remaining-data-free methods significantly, with the added advantage of notable computational efficiency. Moreover, due to its principled forgetting mechanism, MU-Mis exhibits stable and effective behavior in sequential unlearning, whereas existing methods are disclosed to exhibit several deficiencies. Collectively, these results underscore the practicality and reliability of MU-Mis for real-world deployment.

Our key contributions can be summarized as follows:

- ❶ We theoretically and empirically reveal that a sample’s contribution is reflected in the amplified sensitivity gap between the target logit and irrelevant logits, enabling the identification of sample contribution with only the pre-trained model.
- ❷ Based on the above analysis and findings, we propose MU-Mis, which suppresses the sample’s contribution by minimizing the sensitivity magnitude gap for the forgetting data.
- ❸ Comprehensive experiments demonstrate the effectiveness and efficiency of MU-Mis. To our best knowledge, it is the first time that a remaining-data-free method can **perform on par with top performing remaining-data-dependent methods**.

## 2 RELATED WORK

The primary goal of machine unlearning (MU) (Shaik et al., 2023; Xu et al., 2024; Bourtoule et al., 2021) is to remove the influence of specific data points on a pre-trained model, protecting data privacy. MU can be categorized into two types (Shaik et al., 2023): *exact* MU and *approximate* MU. Exact MU approaches *parameters* of the retrained model and guarantees the privacy risk statistically(Guo et al., 2020; Suriyakumar & Wilson, 2022; Neel et al., 2021; Giordano et al., 2019; Koh & Liang, 2017), while approximate MU is proposed to approach the *output distribution* of the retrained model.

108 In this paper, we concentrate on approximate unlearning, as it is more practical in large-scale models  
 109 and situations with limited time and resources.

110 **MU by Gradient-Based Update.** One straightforward way to retrieve sample contribution is to keep  
 111 and utilize the historical information (e.g. parameters and gradients) during the training process.  
 112 Graves et al. (Graves et al., 2021) withdraw gradient updates of related batches, and Wu et al. (Wu  
 113 et al., 2020) utilize intermediate checkpoints and quasi-newton method for rapid retraining. The  
 114 requirement of storing historical information raises memory concerns. Another line of work estimates  
 115 the contribution of the forgetting data on learned model parameters through influence function (Koh &  
 116 Liang, 2017), initially introduced to unlearning by Guo et al. (Guo et al., 2020). However, calculating  
 117 the inverse Hessian in influence function is computationally expensive for DNNs and follow-up  
 118 studies are devoted to reducing the computation (Mehta et al., 2022; Peste et al., 2021; Meng et al.,  
 119 2022). While influence-based unlearning shows potential, the withdrawal still hurts performance  
 120 on the remaining data (Wu et al., 2022). Moreover, the influence function is revealed to be fragile  
 121 in DNNs (Basu et al., 2020; Bae et al., 2022; Hammoudeh & Lowd, 2024) due to its reliance on  
 122 the assumptions of convexity and optimality. Existing data influence estimations for DNNs (Hara  
 123 et al., 2019; Pruthi et al., 2020; Chen et al., 2021; Hammoudeh & Lowd, 2024) all require retracing  
 124 the training trajectory and cannot be optimized and applied to MU. In this paper, we shift sample  
 125 contribution from parameter space to function space, *i.e.*,  $\Delta w$  to  $\partial A / \partial x$ , and theoretically indicate  
 126 that sample contributions will be approximately reflected in the sensitivity of the pre-trained model to  
 127 input samples, opening up a new perspective to view sample contribution in DNNs.

128 **MU by loss guided re-optimization.** Above gradient-based unlearning methods suffer from practical  
 129 limitations for DNNs. Generally, practical MU methods unlearn by fine-tuning the model to optimize  
 130 a proposed loss. They typically follow two design ideas: one is to make model’s behavior on the  
 131 forgetting data similar to that on unseen data through knowledge distillation (Chundawat et al., 2023;  
 132 Lin et al., 2023; Kurmanji et al., 2023) or label confusion (Graves et al., 2021; Fan et al., 2024b),  
 133 the other is to suppress the part of parameters that are responsible for predictions of the forgetting  
 134 data (Liu et al., 2024; Foster et al., 2024a; Fan et al., 2024b). However, due to the lack of identifying  
 135 “what to unlearn”, above removal is done either in an “impair-then-repair” regime (Tarun et al., 2023)  
 136 or through specifically designed mechanisms (Hoang et al., 2024; Foster et al., 2024b; Fan et al.,  
 137 2024b) to alleviate the damage. In contrast, we pursue a more principled forgetting operation by  
 138 explicitly identifying sample contributions, which eliminates the need for compensatory procedures.

139 **Remaining-data-free MU.** Developing remaining-data-free methods aligns more closely with the  
 140 essence and practical demands of MU, given the limited accessibility of retained data and the need for  
 141 efficiency in practice. JiT (Foster et al., 2024a) proposes to smooth the output around the forgetting  
 142 data by minimizing local Lipschitz value. While SCAR (Bonato et al., 2024) distills knowledge  
 143 from the pre-trained model and utilizes Out-of-distribution (OOD) data as a surrogate to preserve  
 144 model utility. However, both approaches have an obvious performance gap to SoTA remaining-data-  
 145 dependent methods, and SCAR still relies on additional OOD data. Remaining-data-free unlearning  
 146 is essentially about developing a more principled forgetting mechanism, and we achieve a more  
 147 nuanced removal by identifying sample contribution.

### 148 3 MACHINE LEARNING, MACHINE UNLEARNING AND INPUT SENSITIVITY

#### 149 3.1 PROBLEM FORMULATION

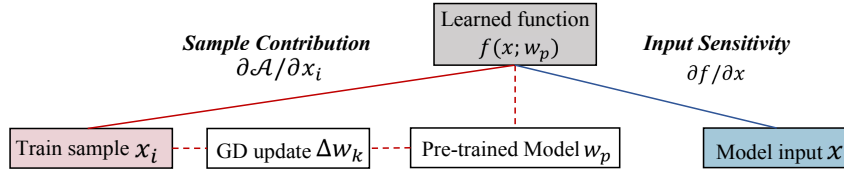
150 **Machine Learning (ML)** is to learn a mapping from the input space  $\mathcal{X}$  to the output space  $\mathcal{Y}$ , denoted  
 151 as the function  $f(\cdot) : \mathcal{X} \rightarrow \mathcal{Y}$ . As we mainly focus on classification models, the output of  $f$  is  
 152 C-dimensional in a C-category classification model. Learning is performed by a *training algorithm*  
 153  $\mathcal{A}$ , which generally takes in a training dataset  $\mathcal{D}$  and returns the *learned function*  $f$ , *i.e.*, the outcome  
 154 of  $\mathcal{A}$  varies with different training datasets. To investigate sample-wise influence on the learning  
 155 process, we consider  $\mathcal{A}$  in a broader sense and distinguish different training processes by the *training*  
 156 *dataset*  $\mathcal{D} = \{(\mathbf{x}_i, \mathbf{y}_i)\}_{i=1}^m$ . That is to say, we have a family of the training algorithm  $\mathcal{A}_{\mathcal{D}}$  and each  
 157 one is a multivariate function that takes all the samples  $\{\mathbf{x}_j \in \mathcal{X}\}$  as input, regardless of whether  
 158 they are in the training dataset  $\mathcal{D}$ . Therefore, the output of  $\mathcal{A}_{\mathcal{D}}$  does not vary with each input variable,  
 159 but only varies with the change of the training data  $\mathbf{x}_i \in \mathcal{D}$ , and makes no response to the change of  
 160 samples out of the training set.

162 **Machine Unlearning (MU)** is to remove the influence of *forgetting data*  $\mathcal{D}_f \subset \mathcal{D}$  from the *pre-trained model*  $w_p$ , while preserving model utility on the *remaining data*  $\mathcal{D}_r = \mathcal{D} \setminus \mathcal{D}_f$ . The learned function  $f$  is parameterized by parameters  $w \in \mathbb{R}^d$  with input variable  $\mathbf{x}$ , *i.e.*, instantiated as  $f(\mathbf{x}; w)$ . A good approximate unlearning mechanism should efficiently and effectively transform  $w_p$  into a *sanitized model*  $w_u$ , such that the output distribution of  $w_u$  closely matches *retrained model*  $w_r$ .

167 **Remark on notation.** To facilitate the understanding of the objectives in our analysis, we only bold 168 the input variables of the training algorithm  $\mathcal{A}_D$  and learned function  $f(\mathbf{x})$ , which are respectively 169  $\mathbf{x}_i$  and  $\mathbf{x}$  in the following analysis.

### 171 3.2 THEORETICAL ANALYSIS CONNECTING SAMPLE CONTRIBUTION AND INPUT SENSITIVITY

173 As previously discussed, machine unlearning is to withdraw sample’s contribution to the learning 174 process, and an efficient unlearning method should explore the contribution directly from the pre- 175 trained model. To detach per-sample contribution with the pre-trained model, we propose to identify 176 the clue of contribution from the derivative of training mapping  $\mathcal{A}_D$  to training sample  $\mathbf{x}_i$ , *i.e.* 177  $\partial \mathcal{A}_D / \partial \mathbf{x}_i$ . Recall that  $\mathcal{A}_D$  is determined by the training dataset  $\mathcal{D} = \{(\mathbf{x}_i, \mathbf{y}_i)\}_{i=1}^m$  and outputs the 178 learned function  $f(\mathbf{x}; w_p)$ . Then  $\partial \mathcal{A}_D / \partial \mathbf{x}_i$  is to compute  $\partial f(\mathbf{x}; w_p) / \partial \mathbf{x}_i$ . However, there is no 179 explicit expression for this derivative. Therefore, in this part, we reflect on the learning dynamics 180 to seek a surrogate with the pre-trained model. Figure 1 provides an overview of the key objectives 181 investigated in our following analysis.



188 **Figure 1: A brief overview of the theoretical connection between sample’s contribution and a**  
189 **pre-trained model’s input sensitivity.** The dashed arrows illustrate how the influence of a training  
190 sample propagates through gradient updates to the pre-trained model.

191 **Gradient Descent (GD).** After  $T$  iterations training updates in the parameter space, we have pre- 192 trained model parameter  $w_p = w_0 + \sum_{k=1}^T \Delta w_k$ , where  $w_0$  is randomly initialized model parameters 193 and  $\Delta w_k = w_{k+1} - w_k$  is the  $k^{\text{th}}$  parameter update. Specifically, when training loss  $\mathcal{L}$  and gradient 194 descent with step size  $\eta$  are used, we have

$$196 \Delta w_k = -\eta \sum_{i=1}^m \frac{\partial \mathcal{L}(\mathbf{x}_i)}{\partial w} \Big|_{w=w_k} = -\eta \sum_{i=1}^m \frac{\partial f(\mathbf{x}_i; w)}{\partial w} \Big|_{w=w_k} \frac{\partial \mathcal{L}(\mathbf{x}_i)}{\partial f}.$$

199 **Function space update induced by GD.** Viewing machine learning from the function space with 200 first-order Taylor expansion on parameters, correspondingly we have  $f = f_0 + \sum_{k=1}^T \Delta f_k$ , where 201  $f_0 = f(\mathbf{x}, w_0)$  is initial function and  $\Delta f_k$  is induced by parameter update  $\Delta w_k$ . The evolution in 202 function induced by parameter update is:

$$203 \Delta f_k(\mathbf{x}; w) \approx \frac{\partial f(\mathbf{x}; w)}{\partial w} \Big|_{w=w_k}^\top \Delta w_k = -\eta \sum_{i=1}^m \frac{\partial f(\mathbf{x}; w)}{\partial w} \Big|_{w=w_k}^\top \frac{\partial f(\mathbf{x}_i; w)}{\partial w} \Big|_{w=w_k} \frac{\partial \mathcal{L}(\mathbf{x}_i)}{\partial f}.$$

206 **Learned function.** To better explain the idea, we make simplifications: *(i)* Note that  $\frac{\partial f(\cdot; w)}{\partial w} \Big|_{w=w_k}$  is 207 the mapping from model input  $\mathbf{x}$  to the induced backpropagation gradient with parameters  $w_k$ . We 208 abbreviate this mapping as  $g_k(\mathbf{x}) : \mathcal{X} \rightarrow \mathbb{R}^{d \times C}$  and its derivative to input  $\mathbf{x}$  as  $g'_k$ , where  $d$  is total 209 number of model parameters. *(ii)* In classification problem with cross-entropy loss as  $\mathcal{L}$ , we have 210  $\frac{\partial \mathcal{L}(\mathbf{x}_i)}{\partial f} = e_c - p(\mathbf{x}_i)$ , where  $e_c$  is a one-hot vector with only  $c^{\text{th}}$  element equals to 1, and  $p$  is the 211 probability vector of  $\mathbf{x}_i$ . The final learned function  $f$  is 212

$$213 f(\mathbf{x}; w_p) = f(\mathbf{x}; w_0) + \sum_{k=1}^T \Delta f_k(\mathbf{x}, w) = f(\mathbf{x}; w_0) - \eta \sum_{k=1}^T \underbrace{g_k^\top(\mathbf{x})}_{(1)} \underbrace{\sum_{i=1}^m g_k(\mathbf{x}_i) (e_c - p(\mathbf{x}_i))}_{(2)}.$$

Notice that term (1) is related to the **forward inference process** while term (2) is related to the **machine learning process**. Derivative of  $f$  w.r.t  $\mathbf{x}$  indicates how the prediction of  $f$  varies with its input  $\mathbf{x}$  at inference time, while derivative w.r.t  $\mathbf{x}_i$  indicates how the learned function  $f$  varies when the training sample  $\mathbf{x}_i$  varies. The former implies **the learned model's sensitivity to its input**, and the latter is **the training sample's influence on learning**. Next, we take the derivative of  $f$  w.r.t  $\mathbf{x}$  and  $\mathbf{x}_i$  respectively to view their relationship. Note that  $p$  is a probability vector determined by  $\mathbf{x}_i$ . Due to softmax activation, we consider  $p(\mathbf{x}_i)$  hardly changes around  $\mathbf{x}_i$ , and omit its derivative term w.r.t  $\mathbf{x}_i$ . The difference in mapping  $g_k$  when  $\mathbf{x}_i$  changes is also omitted.

$$\begin{cases} \frac{\partial f(\mathbf{x}; w_p)}{\partial \mathbf{x}_i} = -\eta \sum_{k=1}^T \underbrace{g'_k(\mathbf{x}_i) g_k(\mathbf{x}) (e_c - p(\mathbf{x}_i))}_{=: \mathcal{C}_k(\mathbf{x}, \mathbf{x}_i)}, \\ \frac{\partial f(\mathbf{x}; w_p)}{\partial \mathbf{x}} = \frac{\partial f(\mathbf{x}; w_0)}{\partial \mathbf{x}} - \eta \sum_{k=1}^T \sum_{i=1}^m \underbrace{g'_k(\mathbf{x}) g_k(\mathbf{x}_i) (e_c - p(\mathbf{x}_i))}_{=: \mathcal{S}_k(\mathbf{x}, \mathbf{x}_i)}. \end{cases} \quad (1)$$

**Input sensitivity of learned function reflects sample contribution.**  $\mathcal{C}_k(\mathbf{x}, \mathbf{x}_i)$  determines the prediction change on  $\mathbf{x}$  when  $\mathbf{x}_i$  changes, and  $\mathcal{S}_k(\mathbf{x}, \mathbf{x}_i)$  stands for the part of model's sensitivity to  $\mathbf{x}$  contributed by training sample  $\mathbf{x}_i$ . Note that  $\frac{\partial f(\mathbf{x}_i; w_p)}{\partial \mathbf{x}_i}$  is similar to the definition of memorization, which is framed as *self-influence* (Feldman, 2020; Feldman & Zhang, 2020). To be more specific, memorization of a sample is defined as the prediction difference in itself when training with or without it. Similarly, the self-influence here is the prediction difference on  $\mathbf{x}_i$  when it slightly changes, i.e.  $\frac{\partial f(\mathbf{x}_i; w_p)}{\partial \mathbf{x}_i}$ . Thus we consider  $\frac{\partial f(\mathbf{x}_i; w_p)}{\partial \mathbf{x}_i}$  as the reflection of sample  $\mathbf{x}_i$ 's contribution. From the formulation, we have  $\mathcal{S}_k(\mathbf{x}_i, \mathbf{x}_i) = \mathcal{C}_k(\mathbf{x}_i, \mathbf{x}_i)$ . For a specific training sample  $\hat{\mathbf{x}} \in \mathcal{D}$ , the learned model's sensitivity to it can be further decomposed as

$$\begin{aligned} \frac{\partial f(\mathbf{x}; w_p)}{\partial \mathbf{x}}|_{\mathbf{x}=\hat{\mathbf{x}}} &= \frac{\partial f(\mathbf{x}; w_0)}{\partial \mathbf{x}}|_{\mathbf{x}=\hat{\mathbf{x}}} - \eta \sum_{k=1}^T \sum_{i=1}^m \mathcal{S}_k(\hat{\mathbf{x}}, \mathbf{x}_i) \\ &= \frac{\partial f(\mathbf{x}, w_0)}{\partial \mathbf{x}}|_{\mathbf{x}=\hat{\mathbf{x}}} - \eta \sum_{k=1}^T \left[ \mathcal{S}_k(\hat{\mathbf{x}}, \hat{\mathbf{x}}) + \sum_{\tilde{\mathbf{x}} \in \mathcal{D} / \hat{\mathbf{x}}} \mathcal{S}_k(\hat{\mathbf{x}}, \tilde{\mathbf{x}}) \right] \\ &= \underbrace{-\eta \sum_{k=1}^T \mathcal{S}_k(\hat{\mathbf{x}}, \hat{\mathbf{x}})}_{\text{Contribution Term}} + \underbrace{\frac{\partial f(\mathbf{x}, w_0)}{\partial \mathbf{x}}|_{\mathbf{x}=\hat{\mathbf{x}}} - \eta \sum_{k=1}^T \sum_{\tilde{\mathbf{x}} \in \mathcal{D} / \hat{\mathbf{x}}} \mathcal{S}_k(\hat{\mathbf{x}}, \tilde{\mathbf{x}})}_{\text{Residual Term}}. \end{aligned} \quad (2)$$

The randomly initialized function  $f_0$  is generally quite insensitive to input change. Thus, the first term of the above residual term is very small. The second term is related to the correlation between the gradient on  $\tilde{\mathbf{x}}$  and the sensitivity of the gradient on  $\hat{\mathbf{x}}$ . We use a simple MLP model to illustrate the insight of  $\mathcal{S}_k(\hat{\mathbf{x}}, \tilde{\mathbf{x}}) \ll \mathcal{S}_k(\hat{\mathbf{x}}, \hat{\mathbf{x}})$  with  $\hat{\mathbf{x}} \neq \tilde{\mathbf{x}}$  in Appendix D. Therefore, the residual term is relatively smaller than the contribution term. In summary, the contribution of a training sample to the training process would be approximately reflected in the pre-trained model's output sensitivity to the sample.

**Empirical validation.** We validate the contribution to learning by comparing  $\|\nabla_{\mathbf{x}} f\|_F$  of the training data before and after training in Figure 2. In a randomly initialized model, there is little response to input changes, only about  $10^{-4}$ . After training, there is a significant order of magnitude growth to  $10^3$ , indicating an increased attention of the trained model to the training data's variations. This implies that the training data contribute to model performance, and such efforts include promoting the model's sensitivity to them during training.

### 3.3 INPUT SENSITIVITY OF THE TARGET AND IRRELEVANT CLASS LOGIT

During training, model predictions on samples are driven toward their correct labels, so sample contributions might differ across logits. To further refine our view of sample contribution, we examine individual logits of  $f(\mathbf{x}) \in \mathbb{R}^C$  in the following part.

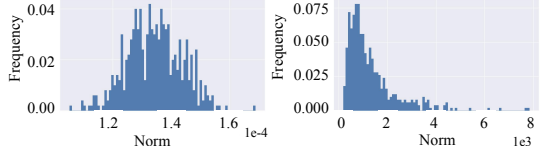


**Figure 2: Input sensitivity  $\|\nabla_{\mathbf{x}} f\|_F$  of training data before and after training.** Left: In randomly initialized model  $w_0$ . Right: In well-trained model  $w_p$ . After training, the model exhibits significantly increased sensitivity to the training data, reflecting their contribution during training.

270 Let  $f_c$  denotes the logit output of the target  
 271 class and  $f_{c'}$  denotes the logit output of irrele-  
 272 vant classes. Figure 3 compares distributions  
 273 between  $\|\nabla_x f_c\|_F$  and  $\frac{1}{C-1} \sum_{c' \neq c} \|\nabla_x f_{c'}\|_F$   
 274 (denoted as  $\|\nabla_x f_{c'}\|_F$  for brevity in the fol-  
 275 lowing) of training data before and after train-  
 276 ing. In the **randomly initialized** model, these  
 277 two quantities are of **comparative magnitude**, but  $\|\nabla_x f_c\|_F$  becomes **much larger**  
 278 than  $\|\nabla_x f_{c'}\|_F$  **after training**. This observa-  
 279 tion implies that samples contribute to ampli-  
 280 fying  $\|\nabla_x f_c\|_F$  to surpass  $\|\nabla_x f_{c'}\|_F$  during  
 281 training, generating a discernible difference in  
 282 whether a sample has been learned. A complemen-  
 283 tary explanation of this finding comes from the  
 284 generative view of discriminative models: the softmax-based discriminative classifier is revealed to  
 285 be implicitly a density model which learns data distribution (Grathwohl et al.; Srinivas & Fleuret,  
 286 2021). From this viewpoint, the logits  $f(\mathbf{x})$  of standard classifiers are un-normalized log-densities,  
 287 and corresponding input-gradients  $\nabla_x f_i(\mathbf{x})$  are log-gradients of a class-conditional density model.  
 288 In other words, we have  $\nabla_{\mathbf{x}} \log p_{\theta}(\mathbf{x}|y=i) = \nabla_x f_i(\mathbf{x})$  in the classification model, providing a  
 289 rationale for the observed discrepancy.

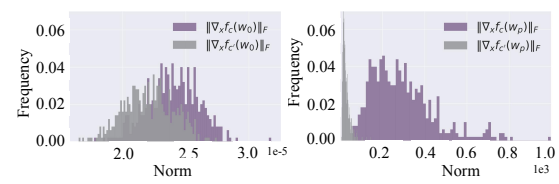


Figure 3: **Input sensitivity**  $\|\nabla_x f_c\|_F$  and  $\|\nabla_x f_{c'}\|_F$  **before and after training**. Left: randomly initialized model  $w_0$ . Right: well-trained model  $w_p$ . After training, the gap between target and irrelevant class sensitivities enlarges, providing a clearer signal of the sample’s contribution.

### 290 3.4 INPUT SENSITIVITY OF SAMPLES PRESENT AND ABSENT IN TRAINING

291 For effective unlearning, the optimization objective should accurately steer the pre-trained model  
 292 toward the retrained model. To validate that the theoretically grounded sensitivity gap provides  
 293 a reliable measure of sample contribution to guide unlearning, we empirically examine the input  
 294 sensitivity of forgetting data under MU scenarios (introduced in Section 5.1 and Appendix F.1).

295 For each forgetting sample, we compute the difference  $\Delta$  between the retrained and the pre-trained  
 296 model’s sensitivity to it, where the sensitivity including  $\|\nabla_x f_c\|_F$ ,  $\|\nabla_x f_{c'}\|_F$  and  $\|\nabla_x f_c\|_F -$   
 297  $\|\nabla_x f_{c'}\|_F$ . Aiming for a light-weight unlearning algorithm, we prefer an optimization direction  
 298 rather than modeling a distribution or specifying a target value for each sample. Hence, we focus on  
 299 the *sign* of  $\Delta$  and count the ratio of rise and fall of  $\Delta$  to examine the overall trend in Figure 4.

300 From left to right in Figure 4,  $\Delta$  is the sample-wise difference between the retrained and pre-trained  
 301 model on  $\|\nabla_x f_c\|_F$ ,  $\|\nabla_x f_{c'}\|_F$  and  $\|\nabla_x f_c\|_F - \|\nabla_x f_{c'}\|_F$ . For each quantity, there is a consistent  
 302 trend across different unlearning settings. Generally,  $f_c$  of the retrained model exhibits lower  
 303 sensitivity and  $f_{c'}$  exhibits higher sensitivity to the forgetting data than the pre-trained model. And  
 304 their sensitivity magnitude gap is consistently smaller in the retrained model across different settings.  
 305 Therefore, the sensitivity magnitude gap faithfully reflects the behavior of the retrained model and  
 306 thus serves as a reliable objective to guide unlearning.



307 Figure 4: **Ratio of input sensitivity difference  $\Delta$  rise and fall of the forgetting data under**  
 308 **different unlearning settings**. From left to right,  $\Delta$  is the sample-wise difference between the  
 309 retrained and pre-trained model on  $\|\nabla_x f_c\|_F$ ,  $\|\nabla_x f_{c'}\|_F$  and  $\|\nabla_x f_c\|_F - \|\nabla_x f_{c'}\|_F$ . Sample’s  
 310 contribution to input sensitivity includes promoting  $\|\nabla_x f_c\|_F$  and suppressing  $\|\nabla_x f_{c'}\|_F$ , thereby  
 311 enlarging the magnitude gap  $\|\nabla_x f_c\|_F - \|\nabla_x f_{c'}\|_F$ .

## 321 4 PROPOSED METHOD

### 322 4.1 MU-MIS: MACHINE UNLEARNING BY MINIMIZING INPUT SENSITIVITY

In the above section, we theoretically and empirically derived an optimizable and lightweight approximation of sample contributions from the perspective of input sensitivity, showing that they manifest as disproportionately higher sensitivity of the target logit relative to irrelevant logits.

In light of this finding, we propose to withdraw the sample’s contribution by reducing such enhancement on the sensitivity magnitude gap. Minimizing this loss guides the pre-trained model to roll back  $\|\nabla_x f_c\|_F$  and pick up  $\|\nabla_x f_{c'}\|_F$ . Mathematically, our proposed unlearning loss is:

$$\mathcal{L}(\mathcal{D}_f; w) = \frac{1}{N_f} \sum_{x_f \in \mathcal{D}_f} (\|\nabla_x f_c(x_f, w)\|_F^2 - \|\nabla_x f_{c'}(x_f, w)\|_F^2) \quad (3)$$

where  $N_f$  is number of the forgetting data,  $c$  represents the target class of sample  $x$  and  $c' \neq c$  denotes an irrelevant class. For each forgetting sample, a new  $c'$  is randomly selected every time the loss is computed.

**Stopping Guideline.** To ensure a practical deployment of MU-Mis, we design a stopping rule for terminating optimization once the withdrawal is completed. Empirical analysis in Appendix E reveals a consistent trend of metrics during our optimization: as the MU-Mis loss decreases, forgetting accuracy (FA) drops steadily, while the accuracies on retained (RA) and test data (TA) initially decline slightly and then grow with the recovery of irrelevant-class logit sensitivity. Crucially, RA approaches the retrained model when this sensitivity returns to its initial level. Therefore, we introduce a threshold ratio  $\delta$  to govern the termination of unlearning. This criterion ensures that optimization halts when irrelevant-class sensitivity is sufficiently restored. The overall algorithm is outlined in Algorithm 1.

## 5 EXPERIMENTS

### 5.1 EXPERIMENT SETUPS

**Tasks, Datasets and Models.** We evaluate unlearning across 3 settings: full-class (CIFAR-100 (Krizhevsky et al., 2009), PinsFaceRecognition (Burak, 2020), and Tiny ImageNet (Le & Yang, 2015)), sub-class (CIFAR-20 (Krizhevsky et al., 2009)), and random-subset (CIFAR-10 (Krizhevsky et al., 2009) and SVHN (Netzer et al., 2011)). ResNet-18 (He et al., 2016) is adopted as the default backbone, and we additionally evaluate under ViT (Dosovitskiy et al., 2021) to highlight the efficiency of remaining-data-free methods. Beyond unlearning utility, we assess the resilience of unlearning methods by executing multiple full-class and sub-class unlearning requests iteratively.

**Evaluation Metrics.** MU methods should be assessed from three aspects (Xu et al., 2024): *utility*, *privacy*, and *efficiency*. For *utility*, we compute forgetting data accuracy (FA), remaining data accuracy (RA), and test data accuracy (TA) of the unlearned model. The average gap (**Avg. Gap**) between the retrained model and the unlearned model across above 3 accuracy-related metrics are computed to illustrate the utility disparity. We compute the train (**FGTA**) and valid (**FGVA**) accuracy on the forgotten classes in sequential unlearning. *Regarding the privacy guarantee, we use 2 complementary membership inference attack (MIA) methods, MIA-Entropy (Chundawat et al., 2023) and MIA-SCRUB (Kurmanji et al., 2023) to probe the remaining information of the forgetting data.* For *efficiency*, we provide the run time efficiency (**RTE**) in **seconds** to indicate timeliness.

**Baselines.** We compare against 8 remaining-data methods: Bad Teacher(BT) (Chundawat et al., 2023), Fine-tune(FT) (Warnecke et al., 2023), SCRUB (Kurmanji et al., 2023), SSD (Foster et al., 2024b), DUCK (Cotogni et al., 2023), SalUn (Fan et al., 2024b), MUNBa (Wu & Harandi, 2025) and LoTus (Spartalis et al., 2025), as well as 4 remaining-data-free methods: RL (Golatkar et al., 2020), NG (Thudi et al., 2022), JiT (Foster et al., 2024a), SCAR (Bonato et al., 2024). Notably, unlike SCAR, our method requires no auxiliary OOD data. Further details on sequential unlearning settings, metrics, and baselines are provided in Appendix F.1.

---

### Algorithm 1 MU-Mis: Machine Unlearning by Minimizing Input Sensitivity

---

**Input:** Forgetting data  $\mathcal{D}_f$ ; Pre-trained model weights  $w_p$ ; Learning rate  $\eta$ ; Stopping threshold ratio  $\delta$ .

**# Initialization**

1:  $w_0 \leftarrow w_p, \epsilon \leftarrow \infty$

**# Iterative optimization**

2: **repeat**

3:   **for** each forgetting sample  $x \in \mathcal{D}_f$  **do**

4:     Randomly select an irrelevant class  $c' \neq c$

5:   **end for**

6:   Compute loss  $\mathcal{L}$  according to equation 3

7:   Update  $w_{t+1} \leftarrow w_t - \eta \nabla \mathcal{L}$

8:   Update  $\epsilon \leftarrow \min(\epsilon, \|\nabla_x f_{c'}(x, w_t)\|_F)$

9: **until**  $\|\nabla_x f_{c'}(x, w_t)\|_F > \epsilon$  **and**

$$\frac{\|\nabla_x f_{c'}(x, w_t)\|_F}{\|\nabla_x f_{c'}(x, w_0)\|_F} > \delta$$

**Output:** Updated model weights  $w_t$

---

500  
501  
502  
503  
504  
505  
506  
507  
508  
509  
510  
511  
512  
513  
514  
515  
516  
517  
518  
519  
520  
521  
522  
523  
524  
525  
526  
527  
528  
529  
530  
531  
532  
533  
534  
535  
536  
537  
538  
539  
540  
541  
542  
543  
544  
545  
546  
547  
548  
549  
550  
551  
552  
553  
554  
555  
556  
557  
558  
559  
560  
561  
562  
563  
564  
565  
566  
567  
568  
569  
570  
571  
572  
573  
574  
575  
576  
577  
578  
579  
580  
581  
582  
583  
584  
585  
586  
587  
588  
589  
590  
591  
592  
593  
594  
595  
596  
597  
598  
599  
600  
601  
602  
603  
604  
605  
606  
607  
608  
609  
610  
611  
612  
613  
614  
615  
616  
617  
618  
619  
620  
621  
622  
623  
624  
625  
626  
627  
628  
629  
630  
631  
632  
633  
634  
635  
636  
637  
638  
639  
640  
641  
642  
643  
644  
645  
646  
647  
648  
649  
650  
651  
652  
653  
654  
655  
656  
657  
658  
659  
660  
661  
662  
663  
664  
665  
666  
667  
668  
669  
670  
671  
672  
673  
674  
675  
676  
677  
678  
679  
680  
681  
682  
683  
684  
685  
686  
687  
688  
689  
690  
691  
692  
693  
694  
695  
696  
697  
698  
699  
700  
701  
702  
703  
704  
705  
706  
707  
708  
709  
710  
711  
712  
713  
714  
715  
716  
717  
718  
719  
720  
721  
722  
723  
724  
725  
726  
727  
728  
729  
730  
731  
732  
733  
734  
735  
736  
737  
738  
739  
740  
741  
742  
743  
744  
745  
746  
747  
748  
749  
750  
751  
752  
753  
754  
755  
756  
757  
758  
759  
760  
761  
762  
763  
764  
765  
766  
767  
768  
769  
770  
771  
772  
773  
774  
775  
776  
777  
778  
779  
780  
781  
782  
783  
784  
785  
786  
787  
788  
789  
790  
791  
792  
793  
794  
795  
796  
797  
798  
799  
800  
801  
802  
803  
804  
805  
806  
807  
808  
809  
810  
811  
812  
813  
814  
815  
816  
817  
818  
819  
820  
821  
822  
823  
824  
825  
826  
827  
828  
829  
830  
831  
832  
833  
834  
835  
836  
837  
838  
839  
840  
841  
842  
843  
844  
845  
846  
847  
848  
849  
850  
851  
852  
853  
854  
855  
856  
857  
858  
859  
860  
861  
862  
863  
864  
865  
866  
867  
868  
869  
870  
871  
872  
873  
874  
875  
876  
877  
878  
879  
880  
881  
882  
883  
884  
885  
886  
887  
888  
889  
890  
891  
892  
893  
894  
895  
896  
897  
898  
899  
900  
901  
902  
903  
904  
905  
906  
907  
908  
909  
910  
911  
912  
913  
914  
915  
916  
917  
918  
919  
920  
921  
922  
923  
924  
925  
926  
927  
928  
929  
930  
931  
932  
933  
934  
935  
936  
937  
938  
939  
940  
941  
942  
943  
944  
945  
946  
947  
948  
949  
950  
951  
952  
953  
954  
955  
956  
957  
958  
959  
960  
961  
962  
963  
964  
965  
966  
967  
968  
969  
970  
971  
972  
973  
974  
975  
976  
977  
978  
979  
980  
981  
982  
983  
984  
985  
986  
987  
988  
989  
990  
991  
992  
993  
994  
995  
996  
997  
998  
999  
1000  
1001  
1002  
1003  
1004  
1005  
1006  
1007  
1008  
1009  
10010  
10011  
10012  
10013  
10014  
10015  
10016  
10017  
10018  
10019  
10020  
10021  
10022  
10023  
10024  
10025  
10026  
10027  
10028  
10029  
10030  
10031  
10032  
10033  
10034  
10035  
10036  
10037  
10038  
10039  
10040  
10041  
10042  
10043  
10044  
10045  
10046  
10047  
10048  
10049  
10050  
10051  
10052  
10053  
10054  
10055  
10056  
10057  
10058  
10059  
10060  
10061  
10062  
10063  
10064  
10065  
10066  
10067  
10068  
10069  
10070  
10071  
10072  
10073  
10074  
10075  
10076  
10077  
10078  
10079  
10080  
10081  
10082  
10083  
10084  
10085  
10086  
10087  
10088  
10089  
10090  
10091  
10092  
10093  
10094  
10095  
10096  
10097  
10098  
10099  
100100  
100101  
100102  
100103  
100104  
100105  
100106  
100107  
100108  
100109  
100110  
100111  
100112  
100113  
100114  
100115  
100116  
100117  
100118  
100119  
100120  
100121  
100122  
100123  
100124  
100125  
100126  
100127  
100128  
100129  
100130  
100131  
100132  
100133  
100134  
100135  
100136  
100137  
100138  
100139  
100140  
100141  
100142  
100143  
100144  
100145  
100146  
100147  
100148  
100149  
100150  
100151  
100152  
100153  
100154  
100155  
100156  
100157  
100158  
100159  
100160  
100161  
100162  
100163  
100164  
100165  
100166  
100167  
100168  
100169  
100170  
100171  
100172  
100173  
100174  
100175  
100176  
100177  
100178  
100179  
100180  
100181  
100182  
100183  
100184  
100185  
100186  
100187  
100188  
100189  
100190  
100191  
100192  
100193  
100194  
100195  
100196  
100197  
100198  
100199  
100200  
100201  
100202  
100203  
100204  
100205  
100206  
100207  
100208  
100209  
100210  
100211  
100212  
100213  
100214  
100215  
100216  
100217  
100218  
100219  
100220  
100221  
100222  
100223  
100224  
100225  
100226  
100227  
100228  
100229  
100230  
100231  
100232  
100233  
100234  
100235  
100236  
100237  
100238  
100239  
100240  
100241  
100242  
100243  
100244  
100245  
100246  
100247  
100248  
100249  
100250  
100251  
100252  
100253  
100254  
100255  
100256  
100257  
100258  
100259  
100260  
100261  
100262  
100263  
100264  
100265  
100266  
100267  
100268  
100269  
100270  
100271  
100272  
100273  
100274  
100275  
100276  
100277  
100278  
100279  
100280  
100281  
100282  
100283  
100284  
100285  
100286  
100287  
100288  
100289  
100290  
100291  
100292  
100293  
100294  
100295  
100296  
100297  
100298  
100299  
100300  
100301  
100302  
100303  
100304  
100305  
100306  
100307  
100308  
100309  
100310  
100311  
100312  
100313  
100314  
100315  
100316  
100317  
100318  
100319  
100320  
100321  
100322  
100323  
100324  
100325  
100326  
100327  
100328  
100329  
100330  
100331  
100332  
100333  
100334  
100335  
100336  
100337  
100338  
100339  
100340  
100341  
100342  
100343  
100344  
100345  
100346  
100347  
100348  
100349  
100350  
100351  
100352  
100353  
100354  
100355  
100356  
100357  
100358  
100359  
100360  
100361  
100362  
100363  
100364  
100365  
100366  
100367  
100368  
100369  
100370  
100371  
100372  
100373  
100374  
100375  
100376  
100377  
100378  
100379  
100380  
100381  
100382  
100383  
100384  
100385  
100386  
100387  
100388  
100389  
100390  
100391  
100392  
100393  
100394  
100395  
100396  
100397  
100398  
100399  
100400  
100401  
100402  
100403  
100404  
100405  
100406  
100407  
100408  
100409  
100410  
100411  
100412  
100413  
100414  
100415  
100416  
100417  
100418  
100419  
100420  
100421  
100422  
100423  
100424  
100425  
100426  
100427  
100428  
100429  
100430  
100431  
100432  
100433  
100434  
100435  
100436  
100437  
100438  
100439  
100440  
100441  
100442  
100443  
100444  
100445  
100446  
100447  
100448  
100449  
100450  
100451  
100452  
100453  
100454  
100455  
100456  
100457  
100458  
100459  
100460  
100461  
100462  
100463  
100464  
100465  
100466  
100467  
100468  
100469  
100470  
100471  
100472  
100473  
100474  
100475  
100476  
100477  
100478  
100479  
100480  
100481  
100482  
100483  
100484  
100485  
100486  
100487  
100488  
100489  
100490  
100491  
100492  
100493  
100494  
100495  
100496  
100497  
100498  
100499  
100500  
100501  
100502  
100503  
100504  
100505  
100506  
100507  
100508  
100509  
100510  
100511  
100512  
100513  
100514  
100515  
100516  
100517  
100518  
100519  
100520  
100521  
100522  
100523  
100524  
100525  
100526  
100527  
100528  
100529  
100530  
100531  
100532  
100533  
100534  
100535  
100536  
100537  
100538  
100539  
100540  
100541  
100542  
100543  
100544  
100545  
100546  
100547  
100548  
100549  
100550  
100551  
100552  
100553  
100554  
100555  
100556  
100557  
100558  
100559  
100560  
100561  
100562  
100563  
100564  
100565  
100566  
100567  
100568  
100569  
100570  
100571  
100572  
100573  
100574  
100575  
100576  
100577  
100578  
100579  
100580  
100581  
100582  
100583  
100584  
100585  
100586  
100587  
100588  
100589  
100590  
100591  
100592  
100593  
100594  
100595  
100596  
100597  
100598  
100599  
100600  
100601  
100602  
100603  
100604  
100605  
100606  
100607  
100608  
100609  
100610  
100611  
100612  
100613  
100614  
100615  
100616  
100617  
100618  
100619  
100620  
100621  
100622  
100623  
100624  
100625  
100626  
100627  
100628  
100629  
100630  
100631  
100632  
100633  
100634  
100635  
100636  
100637  
100638  
100639  
100640  
100641  
100642  
100643  
100644  
100645  
100646  
100647  
100648  
100649  
100650  
100651  
100652  
100653  
100654  
100655  
100656  
100657  
100658  
100659  
100660  
100661  
100662  
100663  
100664  
100665  
100666  
100667  
100668  
100669  
100670  
100671  
100672  
100673  
100674  
100675  
100676  
100677  
100678  
100679  
100680  
100681  
100682  
100683  
100684  
100685  
100686  
100687  
100688  
100689  
100690  
100691  
100692  
100693  
100694  
100695  
100696  
100697  
100698  
100699  
100700  
100701  
100702  
100703  
100704  
100705  
100706  
100707  
100708  
100709  
100710  
100711  
100712  
100713  
100714  
100715  
100716  
100717  
100718  
100719  
100720  
100721  
100722  
100723  
100724  
100725  
100726  
100727  
100728  
100729  
100730  
100731  
100732  
100733  
100734  
100735  
100736  
100737  
100738  
100739  
100740  
100741  
100742  
100743  
100744  
100745  
100746  
100747  
100748  
100749  
100750  
100751  
100752  
100753  
100754  
100755  
100756  
100757  
100758  
100759  
100760  
100761  
100762  
100763  
100764  
100765  
100766  
100767  
100768  
100769  
100770  
100771  
100772  
100773  
100774  
100775  
100776  
100777  
100778  
100779  
100780  
100781  
100782  
100783  
100784  
100785  
100786  
100787  
100788  
100789  
100790  
100791  
100792  
100793  
100794  
100795  
100796  
100797  
100798  
100799  
100800  
100801  
100802  
100803  
100804  
100805  
100806  
100807  
100808  
100809  
100810

378  
379

## 5.2 UNLEARNING UTILITY

380  
381  
382  
383  
384  
385  
386Table 1: Performance overview for **full class** unlearning task evaluated on CIFAR-100 and Tiny ImageNet using ResNet-18. This table includes performances of our proposed MU-Mis, 6 remaining-data-dependent and 4 remaining-data-free methods, which are delineated by a horizontal line. The result format is given by  $a \pm b$  with mean  $a$  and standard deviation  $b$  over 5 independent trials. The metric *average gap* (*Avg. Gap*) is calculated by the average of the performance gaps measured in accuracy-related metrics, including FA, RA and TA. RTE is reported in **seconds**. Values in terms of accuracy-related metrics deviating by more than 5% from the retrain model are highlighted in **red**.

387

Method	CIFAR-100						Tiny ImageNet					
	RA	FA	TA	Avg. Gap $\downarrow$	MIA	RTE	RA	FA	TA	Avg. Gap $\downarrow$	MIA	RTE
Pretrain	76.41	79.69	76.47	26.84	95.80	10880	65.85	62.00	65.50	21.03	93.59	13600
Retrain	76.52 $\pm$ 0.27	0.00 $\pm$ 0.00	75.76 $\pm$ 0.24	0.00	2.87 $\pm$ 0.46	7432	65.36 $\pm$ 0.03	0.00 $\pm$ 0.03	64.90 $\pm$ 0.03	0.00	4.80 $\pm$ 0.04	10367
BT	76.67 $\pm$ 0.03	0.00 $\pm$ 0.00	76.02 $\pm$ 0.03	0.14	0.00 $\pm$ 0.00	32	64.90 $\pm$ 0.01	0.00 $\pm$ 0.00	64.53 $\pm$ 0.01	0.28	0.00 $\pm$ 0.00	240
FT	76.67 $\pm$ 0.21	0.28 $\pm$ 0.62	75.88 $\pm$ 0.22	0.19	0.28 $\pm$ 0.00	250	64.16 $\pm$ 0.26	0.00 $\pm$ 0.00	63.87 $\pm$ 0.22	0.74	4.40 $\pm$ 0.58	262
SCRUB	76.81 $\pm$ 0.04	0.00 $\pm$ 0.00	76.02 $\pm$ 0.04	0.18	5.57 $\pm$ 0.34	124	65.06 $\pm$ 0.04	0.00 $\pm$ 0.00	64.69 $\pm$ 0.03	0.17	14.60 $\pm$ 0.52	860
SSD	76.27 $\pm$ 0.00	0.00 $\pm$ 0.00	75.49 $\pm$ 0.00	0.17	0.00 $\pm$ 0.00	26	65.58 $\pm$ 0.00	0.00 $\pm$ 0.00	65.19 $\pm$ 0.00	0.17	0.00 $\pm$ 0.00	59
DUCK	75.82 $\pm$ 0.18	0.20 $\pm$ 0.45	75.13 $\pm$ 0.17	0.51	0.00 $\pm$ 0.00	100	64.97 $\pm$ 0.14	0.00 $\pm$ 0.00	64.61 $\pm$ 0.14	0.23	2.60 $\pm$ 0.46	55
SalU	76.63 $\pm$ 0.03	1.20 $\pm$ 0.45	75.85 $\pm$ 0.03	0.47	0.00 $\pm$ 0.00	254	65.21 $\pm$ 0.10	0.00 $\pm$ 0.00	64.88 $\pm$ 0.10	0.06	4.40 $\pm$ 0.40	2630
MUNBa	74.09 $\pm$ 0.11	0.00 $\pm$ 0.00	73.40 $\pm$ 0.12	1.60 $\pm$ 0.03	9.30 $\pm$ 0.18	217	64.22 $\pm$ 0.14	0.00 $\pm$ 0.00	63.88 $\pm$ 0.15	0.72 $\pm$ 0.02	7.80 $\pm$ 0.16	897
LoTus	76.48 $\pm$ 0.08	5.00 $\pm$ 0.02	75.87 $\pm$ 0.08	1.72 $\pm$ 0.04	0.00 $\pm$ 0.00	140	65.02 $\pm$ 0.10	0.00 $\pm$ 0.00	64.65 $\pm$ 0.11	0.20 $\pm$ 0.01	0.00 $\pm$ 0.00	182
NG	69.76 $\pm$ 0.01	0.00 $\pm$ 0.00	69.23 $\pm$ 0.01	4.43	0.00 $\pm$ 0.00	2	59.62 $\pm$ 0.00	0.00 $\pm$ 0.00	59.26 $\pm$ 0.00	3.79	1.80 $\pm$ 0.00	3
RL	65.98 $\pm$ 0.12	5.22 $\pm$ 0.45	65.52 $\pm$ 0.11	8.66	0.00 $\pm$ 0.00	12	53.41 $\pm$ 0.00	0.00 $\pm$ 0.00	53.04 $\pm$ 0.01	7.94	2.00 $\pm$ 0.00	10
SCAR	71.33 $\pm$ 0.12	5.61 $\pm$ 0.89	70.66 $\pm$ 0.14	5.29	13.28 $\pm$ 0.67	367	59.98 $\pm$ 0.06	0.00 $\pm$ 0.00	59.62 $\pm$ 0.06	3.55	0.67 $\pm$ 0.12	1052
JIT	65.44 $\pm$ 0.14	3.00 $\pm$ 0.76	64.87 $\pm$ 0.13	8.32	4.44 $\pm$ 0.30	15	53.82 $\pm$ 0.09	0.00 $\pm$ 0.00	53.16 $\pm$ 0.08	7.76	5.29 $\pm$ 0.25	5
MU-Mis	76.42 $\pm$ 0.07	0.00 $\pm$ 0.00	75.64 $\pm$ 0.07	0.07	0.00 $\pm$ 0.00	30	64.95 $\pm$ 0.00	0.00 $\pm$ 0.00	64.85 $\pm$ 0.00	0.15	0.20 $\pm$ 0.00	83

398

399  
400  
401  
402Table 2: Performance overview for **sub-class** unlearning task evaluated on ‘Rocket’ and ‘Sea’ (where the retrain model exhibits different degrees of generalization ability on the unlearned sub-class) of CIFAR-20 using ResNet-18. The content format follows Table 1.

403

Method	Rocket						Sea					
	RA	FA	TA	Avg. Gap $\downarrow$	MIA	RTE	RA	FA	TA	Avg. Gap $\downarrow$	MIA	RTE
Pretrain	85.26	80.73	85.21	26.53	92.89	6910	85.09	97.66	85.21	5.94	91.81	6910
Retrain	84.85 $\pm$ 0.09	2.69 $\pm$ 0.45	84.07 $\pm$ 0.10	0.00	12.06 $\pm$ 0.75	4298	84.60 $\pm$ 0.22	80.93 $\pm$ 2.20	84.61 $\pm$ 0.19	0.00	51.61 $\pm$ 3.60	4298
BT	85.24 $\pm$ 0.02	2.80 $\pm$ 0.45	84.36 $\pm$ 0.02	0.26	0.00 $\pm$ 0.00	27	82.51 $\pm$ 0.00	81.00 $\pm$ 0.00	82.63 $\pm$ 0.00	1.38	15.00 $\pm$ 0.00	47
FT	82.70 $\pm$ 0.19	4.20 $\pm$ 1.30	81.97 $\pm$ 0.12	1.92	5.40 $\pm$ 1.04	138	82.36 $\pm$ 0.29	88.00 $\pm$ 1.41	82.43 $\pm$ 1.60	3.83	58.08 $\pm$ 1.79	417
SCRUB	84.73 $\pm$ 0.13	5.80 $\pm$ 1.30	83.84 $\pm$ 0.13	1.15	13.28 $\pm$ 0.02	113	84.86 $\pm$ 0.10	88.17 $\pm$ 1.72	84.86 $\pm$ 0.13	2.58	57.07 $\pm$ 1.71	113
SSD	84.23 $\pm$ 0.05	2.60 $\pm$ 0.89	83.35 $\pm$ 0.06	0.48	3.76 $\pm$ 0.36	18	84.79 $\pm$ 0.00	78.00 $\pm$ 0.00	84.61 $\pm$ 0.00	1.24	8.00 $\pm$ 0.00	7
DUCK	82.09 $\pm$ 0.33	19.4 $\pm$ 3.28	81.43 $\pm$ 0.35	7.37	32.84 $\pm$ 1.57	58	80.95 $\pm$ 0.19	66.45 $\pm$ 2.30	80.77 $\pm$ 0.19	7.34	54.92 $\pm$ 2.29	68
SalUn	84.82 $\pm$ 0.00	2.99 $\pm$ 1.25	84.00 $\pm$ 0.05	0.13	0.00 $\pm$ 0.00	1042	82.85 $\pm$ 0.00	81.00 $\pm$ 0.00	83.10 $\pm$ 0.00	1.11	13.40 $\pm$ 0.00	63
MUNBa	81.43 $\pm$ 0.13	7.00 $\pm$ 0.05	80.80 $\pm$ 0.12	3.67 $\pm$ 0.06	7.20 $\pm$ 0.14	362	80.64 $\pm$ 0.14	84.00 $\pm$ 0.15	80.66 $\pm$ 0.13	3.66 $\pm$ 0.05	60.00 $\pm$ 0.20	564
LoTus	35.93 $\pm$ 0.21	39.00 $\pm$ 0.18	36.04 $\pm$ 0.20	44.42 $\pm$ 0.35	18.60 $\pm$ 0.18	105	73.12 $\pm$ 0.15	81.00 $\pm$ 0.16	73.39 $\pm$ 0.14	7.59 $\pm$ 0.08	61.20 $\pm$ 0.19	16
NG	62.84 $\pm$ 5.66	5.67 $\pm$ 4.08	62.48 $\pm$ 5.59	15.52	72.70 $\pm$ 1.80	4	80.95 $\pm$ 0.00	75.00 $\pm$ 0.00	80.84 $\pm$ 0.02	4.45	60.00 $\pm$ 0.00	3
RL	60.89 $\pm$ 1.96	6.52 $\pm$ 1.07	60.50 $\pm$ 2.01	17.11	3.70 $\pm$ 0.51	5	80.48 $\pm$ 0.02	77.00 $\pm$ 0.00	80.34 $\pm$ 0.02	4.11	48.70 $\pm$ 0.11	3
SCAR	76.49 $\pm$ 0.22	43.81 $\pm$ 4.44	76.26 $\pm$ 0.23	19.09	28.04 $\pm$ 1.67	442	76.30 $\pm$ 0.15	77.40 $\pm$ 2.71	76.12 $\pm$ 0.19	6.77	51.84 $\pm$ 1.98	434
JIT	59.15 $\pm$ 0.05	4.00 $\pm$ 0.00	58.60 $\pm$ 0.05	17.49	29.03 $\pm$ 0.20	4	51.48 $\pm$ 0.04	7.20 $\pm$ 1.10	51.04 $\pm$ 0.04	46.81	32.20 $\pm$ 0.24	4
MU-Mis	84.28 $\pm$ 0.18	2.91 $\pm$ 1.02	83.50 $\pm$ 0.19	0.49	0.07 $\pm$ 0.25	21	84.35 $\pm$ 0.03	81.00 $\pm$ 2.95	84.33 $\pm$ 0.05	0.20	1.25 $\pm$ 1.85	10

414

**MU-Mis outperforms existing remaining-data-free methods significantly and remains highly competitive with SoTA remaining-data-dependent methods.** Table 1 and Table 2 correspond to MU performances on full-class and sub-class unlearning respectively. More experiment results are referred to Appendix G.1. In terms of unlearning *utility*, MU-Mis achieves the smallest Avg. Gap in full-class-CIFAR-100, full-class-PinsFaceRecognition, sub-class-Sea and sub-class-Lamp unlearning, outperforming all the baseline methods. From the highlighted values in red in the tables, we could see that existing remaining-data-free methods suffer from poor utility preservation. From Table A8, we could see that there is a clear gap between MU-Mis and RUM in when removing mixture of different memorization level samples. But surprisingly, MU-Mis indicates a lowest KL divergence to the retrained model in the forgetting data, indicating a more principled removal than SalUn and RUM. Overall, MU-Mis surpasses strong remaining-data-dependent methods in full-class and sub-class unlearning, falls short of the RUM in the particularly challenging random-subset setting. But importantly, MU-Mis outperforms all existing remaining-data-free methods by a substantial margin across all scenarios. In terms of *privacy*, MIA-Entropy indicates the residual membership of the forgetting data and MIA-SCRUB indicates non-membership of the forgetting data in the unlearned model. We can see that MIA-Entropy remain consistently low and MIA-SCRUB remain consistently to the retrained model in Table A11 cross 3 tasks, collectively demonstrating a successful privacy protection of MU-Mis. In addition to resolving the issue of constrained access to the remaining data, our remaining-data-free method also offers a notable advantage in MU efficiency. In unlearning a full class Tiny ImageNet, MU-Mis is up to 30 $\times$  faster than SalUn, with only 0.09 higher Avg. Gap.

432  
 433  
 434  
 435  
 436  
 437  
 438  
 439  
 440  
 441  
 442  
 443  
 444  
 445  
 446  
 447  
 448  
 449  
 450  
 451  
 452  
 453  
 454  
 455  
 456  
 457  
 458  
 459  
 460  
 461  
 462  
 463  
 464  
 465  
 466  
 467  
 468  
 469  
 470  
 471  
 472  
 473  
 474  
 475  
 476  
 477  
 478  
 479  
 480  
 481  
 482  
 483  
 484  
 485  
**Efficiency advantage is more pronounced on larger scale models.** Table 1 shows the performance when unlearning a full class of Tiny ImageNet under ViT (Dosovitskiy et al., 2021). MU-Mis outperforms other remaining-data-free methods <sup>1</sup> significantly and performs comparably with the most competitive method SalUn in terms of model utility and privacy. The efficiency advantage of MU-Mis becomes markedly pronounced: the unlearning time is reduced from more than **1 hour** to **3 minutes**. We also evaluate subclass-CIFAR20-sea unlearning under ViT and show the results in Table A10, where MU-Mis exhibits the best Avg.Gap and is 20× faster than SalUn.

Table 3: Performance overview for **full class** unlearning task evaluated on **Tiny ImageNet** using ViT. RTE is reported in **minute**.

Methods	RA	FA	TA	Avg. Gap ↓	MIA	RTE (min)
Pretrain	84.21	87.5	84.23	30.44	95.40	-
Retrain	86.35 <sub>±0.17</sub>	0.00 <sub>±0.00</sub>	85.92 <sub>±0.14</sub>	0.00	8.80 <sub>±0.26</sub>	-
SalUn	83.94 <sub>±0.10</sub>	0.00 <sub>±0.00</sub>	83.49 <sub>±0.14</sub>	1.88	0.00 <sub>±0.00</sub>	81
NG	63.12 <sub>±0.00</sub>	0.00 <sub>±0.00</sub>	62.88 <sub>±0.00</sub>	15.28	0.00 <sub>±0.00</sub>	0.21
RL	67.69 <sub>±0.00</sub>	0.00 <sub>±0.00</sub>	67.43 <sub>±0.00</sub>	12.38	0.00 <sub>±0.00</sub>	0.15
MU-Mis	82.13 <sub>±0.24</sub>	0.00 <sub>±0.00</sub>	82.17 <sub>±0.23</sub>	2.69	0.00 <sub>±0.00</sub>	3

### 5.3 UNLEARNING RESILIENCE: SEQUENTIAL MACHINE UNLEARNING

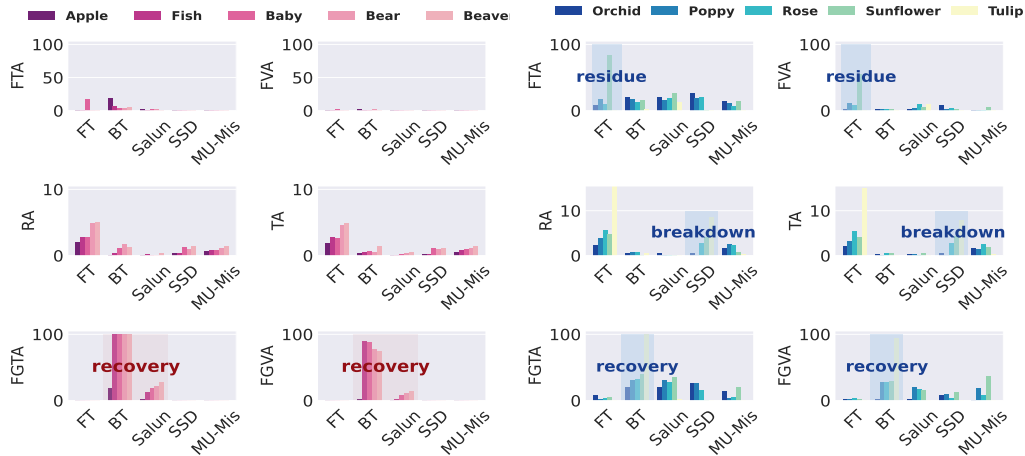


Figure 5: **Disparities in accuracy-related metrics between the unlearned model and the retrained model for full class and sub-class sequential unlearning.** Left: Iteratively unlearns 5 distinct full classes of CIFAR-100. Right: Iteratively unlearns 5 sub-classes of the same super-class ‘Flower’.

**Sequential unlearning requires principled unlearning mechanisms.** In practice, unlearning requests may arrive sequentially, requiring multiple executions of the unlearning method. Wang et al. (2024a) point out that sequential unlearning greatly challenges the memorization management ability of unlearning methods due to underlying associations among unlearned classes. The sequentially unlearned model might break down due to disordered forgetting operation, exposing its accumulated effects on model knowledge. Therefore, to highlight the importance of principled forgetting, we perform sequential unlearning. We examine the impact of subsequent requests on previous unlearning efforts and present the disparities between the unlearned model and the retrain model at each iteration in accuracy-related MU metrics in Figure 5. For detailed experiment settings, refer to Appendix F.1.

**Deficiencies in existing MU methods.** From Figure 5, we can see that there are 3 kinds of deficiencies in existing SoTA MU methods:

(i) *Performance Recovery*. The performance on the forgotten classes stages a recovery in BT and Salun unlearned model, indicated by the above zero FGTA and FGVA. This suggests that retargeting model’s outputs of the forgetting data does not completely remove associated knowledge, posing a substantial risk since the concealed information might still be exploited by privacy attackers.

(ii) *Knowledge Residue*. High disparity of FTA and FVA in sub-class task indicates that FT method, which relies on “catastrophic forgetting” (Kirkpatrick et al., 2017) to unlearn, fails to unlearn effectively in sub-class task due to the resemblance between the forgetting and remaining data.

(iii) *Utility Breakdown*. In sub-class task, SSD exhibits a marked decline in utility after the last unlearning request, demonstrated by the final RA of 76.33%. In contrast, RA in the retrained model

<sup>1</sup>We failed to identify effective hyper-parameters for JiT and SCAR for this experiment.

486 and MU-Mis unlearned model are respectively 84.83% and 84.59%. Such a plummet implies a  
 487 potential risk of model utility breakdowns when the magnitude of parameters is continuously scaled.  
 488

489 **Resilient performance of MU-Mis to sequential  
 490 unlearning requests.** To facilitate an intuitive  
 491 assessment in terms of utility and resilience, we  
 492 compute the utility Avg. Gap and resilience Avg.  
 493 Gap for each iteration in Figure 6. The utility Avg.  
 494 Gap is averaged over FTA, FVA, RA and TA, and  
 495 the resilience Avg. Gap is averaged over FGTA  
 496 and FGVA. From Figure 6, it is evident that MU-  
 497 Mis and SSD are significantly better than BT, FT,  
 498 and Salun, demonstrating a notably small disparity  
 499 to the retrained model regarding both the utility  
 500 and resilience Avg. Gap across the full class and  
 501 sub-class tasks. Importantly, MU-Mis achieves  
 502 these results without relying on the remaining data,  
 503 which are required by SSD.

504 **Minimal KL divergence of MU-Mis from  
 505 retrain model during sequential unlearn.**

506 Beyond model predictions, we further pro-  
 507 vide the empirical KL divergence (intro-  
 508 duced in Appendix F.2) between the  
 509 unlearned model and the retrained model’s  
 510 output distributions during sequential re-  
 511 requests in Figure 7. It is evident that MU-  
 512 Mis exhibits the lowest KL divergence  
 513 from the retrained model throughout both  
 514 the full-class and sub-class sequential un-  
 515 learning processes.

516 **Summary.** In general, MU-Mis stands out with its comprehensive capabilities in terms of unlearning  
 517 utility, unlearning resilience as well as output indistinguishability, while current SoTA MU meth-  
 518 ods are disclosed to exhibit limitations and deficiencies in certain aspects. Their inappropriate or  
 519 inadequate unlearning approaches undermine their reliability and applicability in practical scenarios.

#### 520 5.4 SUPPLEMENTARY EXPERIMENTS AND ANALYSES

521 We provide the following experiments and analyses for completeness in Appendix: (i) ablation  
 522 study of MU-Mis in Appendix G.3; (ii) a hyper-parameter sensitivity analysis showing stability of  
 523 MU-Mis in Appendix G.4; (iii) visualizations of attention map confirming effectiveness of MU-Mis in  
 524 Appendix G.5; (iv) an empirical analysis attributing the effectiveness of MU-Mis to the orthogonality  
 525 of input sensitivity gradients among samples in Appendix H; (vi) A comprehensive analysis covering  
 526 the theoretical link between sensitivity gaps and loss curvature, empirical signatures of sensitivity  
 527 across memorization and influence levels, and the broader role of unlearning in shaping memorization,  
 528 generalization, and sample contribution in Appendix I.

## 529 6 CONCLUSION

531 There are 3 main challenges in machine unlearning: *the stochasticity of training, incrementality*  
 532 *of training*, and *catastrophe of unlearning* (Wang et al., 2024b). We address incrementality by  
 533 quantifying sample contribution through the lens of input sensitivity. Building on this, our proposed  
 534 MU-Mis achieves effective and efficient unlearning without compromising model utility, alleviating  
 535 catastrophic unlearning. Experiments validate the superiority of this principled forgetting mechanism.  
 536 Overall, MU-Mis is well-grounded, lightweight and remaining-data-free, offering a practical and  
 537 competitive alternative to existing unlearning methods. Furthermore, we highlight in Appendix I  
 538 that there is a profound connection between input sensitivity view and machine unlearning, which  
 539 we believe is an interesting direction to further improve remaining-data-free unlearning in the most  
 challenging random subset scenario.



Figure 6: Overview of utility Avg. Gap and resilience Avg. Gap during full class (upper) and sub-class (bottom) sequential unlearning.

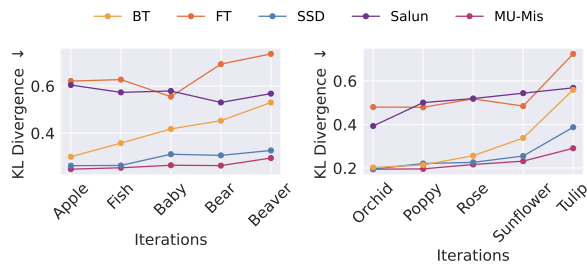


Figure 7: KL divergence between outputs of unlearned model and retrained model during full class (left) and sub-class (right) sequential unlearning.

540 BIBLIOGRAPHY  
541

542 Juhan Bae, Nathan Ng, Alston Lo, Marzyeh Ghassemi, and Roger B Grosse. If influence functions  
543 are the answer, then what is the question? *Advances in Neural Information Processing Systems*  
544 (*NeurIPS*), 35:17953–17967, 2022. 3

545 Samyadeep Basu, Phil Pope, and Soheil Feizi. Influence functions in deep learning are fragile. In  
546 *International Conference on Learning Representations (ICLR)*, 2020. 3

548 Jacopo Bonato, Marco Cotogni, and Luigi Sabetta. Is retain set all you need in machine unlearn-  
549 ing? restoring performance of unlearned models with out-of-distribution images. In *European*  
550 *Conference on Computer Vision (ECCV)*, pp. 1–19. Springer, 2024. 3, 7, 17, 18

552 Lucas Bourtoule, Varun Chandrasekaran, Christopher A Choquette-Choo, Hengrui Jia, Adelin Travers,  
553 Baiwu Zhang, David Lie, and Nicolas Papernot. Machine unlearning. In *2021 IEEE Symposium*  
554 *on Security and Privacy (SP)*, pp. 141–159. IEEE, 2021. 2

555 Burak. Pinterest face recognition dataset. [www.kaggle.com/datasets/hereisburak/pins-facerecognition](http://www.kaggle.com/datasets/hereisburak/pins-facerecognition), 2020. 7, 16

558 Yinzhi Cao and Junfeng Yang. Towards making systems forget with machine unlearning. In *IEEE*  
559 *Symposium on Security and Privacy*, pp. 463–480. IEEE, 2015. 1

560 Nicholas Carlini, Matthew Jagielski, Chiyuan Zhang, Nicolas Papernot, Andreas Terzis, and Florian  
561 Tramer. The privacy onion effect: Memorization is relative. *Advances in Neural Information*  
562 *Processing Systems (NeurIPS)*, 35:13263–13276, 2022. 16

564 Yuanyuan Chen, Boyang Li, Han Yu, Pengcheng Wu, and Chunyan Miao. Hydra: Hypergradient  
565 data relevance analysis for interpreting deep neural networks. In *AAAI Conference on Artificial*  
566 *Intelligence (AAAI)*, volume 35, pp. 7081–7089, 2021. 3

567 Andreas Christmann and Ingo Steinwart. *Support Vector Machines*. Springer, 2008. 2

569 Vikram S Chundawat, Ayush K Tarun, Murari Mandal, and Mohan Kankanhalli. Can bad teaching  
570 induce forgetting? unlearning in deep networks using an incompetent teacher. In *AAAI Conference*  
571 *on Artificial Intelligence (AAAI)*, pp. 7210–7217, 2023. 1, 3, 7, 17, 26

573 Corinna Cortes and Vladimir Vapnik. Support-vector networks. *Machine Learning (ML)*, 20:273–297,  
574 1995. 2

575 Marco Cotogni, Jacopo Bonato, Luigi Sabetta, Francesco Pelosi, and Alessandro Nicolosi. Duck:  
576 Distance-based unlearning via centroid kinematics. *arXiv preprint arXiv:2312.02052*, 2023. 7, 17

578 Alexey Dosovitskiy, Lucas Beyer, Alexander Kolesnikov, Dirk Weissenborn, Xiaohua Zhai, Thomas  
579 Unterthiner, Mostafa Dehghani, Matthias Minderer, Georg Heigold, Sylvain Gelly, Jakob Uszkoreit,  
580 and Neil Houlsby. An image is worth 16x16 words: Transformers for image recognition at scale.  
581 In *9th International Conference on Learning Representations (ICLR)*, 2021. 7, 9

582 Harris Drucker and Yann Le Cun. Improving generalization performance using double backpropaga-  
583 tion. *IEEE Transactions on Neural Networks*, 3(6):991–997, 1992. 26

585 Chongyu Fan, Jiancheng Liu, Alfred Hero, and Sijia Liu. Challenging forgets: Unveiling the worst-  
586 case forget sets in machine unlearning. In *European Conference on Computer Vision*, pp. 278–297.  
587 Springer, 2024a. 28

588 Chongyu Fan, Jiancheng Liu, Yihua Zhang, Eric Wong, Dennis Wei, and Sijia Liu. Salun: Em-  
589 powering machine unlearning via gradient-based weight saliency in both image classification and  
590 generation. In *International Conference on Learning Representations (ICLR)*, 2024b. 1, 3, 7, 17,  
591 26

593 Vitaly Feldman. Does learning require memorization? a short tale about a long tail. In *the Annual*  
594 *ACM SIGACT Symposium on Theory of Computing*, pp. 954–959, 2020. 1, 5, 27

594 Vitaly Feldman and Chiyuan Zhang. What neural networks memorize and why: Discovering the long  
 595 tail via influence estimation. *Advances in Neural Information Processing Systems (NeurIPS)*, 33:  
 596 2881–2891, 2020. 1, 5, 27

597

598 Jack Foster, Kyle Fogarty, Stefan Schoepf, Cengiz Öztureli, and Alexandra Brintrup. Zero-shot  
 599 machine unlearning at scale via lipschitz regularization. *arXiv preprint arXiv:2402.01401*, 2024a.  
 600 3, 7, 17, 18, 26

601 Jack Foster, Stefan Schoepf, and Alexandra Brintrup. Fast machine unlearning without retraining  
 602 through selective synaptic dampening. In *AAAI Conference on Artificial Intelligence (AAAI)*, pp.  
 603 12043–12051, 2024b. 3, 7, 17

604 Isha Garg, Deepak Ravikumar, and Kaushik Roy. Memorization through the lens of curvature of loss  
 605 function around samples. In *International Conference on Machine Learning (ICML)*, 2024. 27

606

607 Ryan Giordano, William Stephenson, Runjing Liu, Michael Jordan, and Tamara Broderick. A swiss  
 608 army infinitesimal jackknife. In *International Conference on Artificial Intelligence and Statistics*,  
 609 pp. 1139–1147. PMLR, 2019. 2

610 Aditya Golatkar, Alessandro Achille, and Stefano Soatto. Eternal sunshine of the spotless net:  
 611 Selective forgetting in deep networks. In *IEEE/CVF Conference on Computer Vision and Pattern  
 612 Recognition (CVPR)*, pp. 9304–9312, 2020. 1, 7, 17, 18

613

614 Will Grathwohl, Kuan-Chieh Wang, Joern-Henrik Jacobsen, David Duvenaud, Mohammad Norouzi,  
 615 and Kevin Swersky. Your classifier is secretly an energy based model and you should treat it like  
 616 one. In *International Conference on Learning Representations (ICLR)*. 6

617 Laura Graves, Vineel Nagisetty, and Vijay Ganesh. Amnesiac machine learning. In *AAAI Conference  
 618 on Artificial Intelligence (AAAI)*, pp. 11516–11524, 2021. 1, 3, 26

619

620 Chuan Guo, Tom Goldstein, Awni Y. Hannun, and Laurens van der Maaten. Certified data removal  
 621 from machine learning models. In *International Conference on Machine Learning (ICML)*, pp.  
 622 3832–3842, 2020. 2, 3

623 Zayd Hammoudeh and Daniel Lowd. Training data influence analysis and estimation: A survey.  
 624 *Machine Learning (ML)*, 113(5):2351–2403, 2024. 3

625

626 Satoshi Hara, Atsushi Nitanda, and Takanori Maehara. Data cleansing for models trained with sgd.  
 627 *Advances in Neural Information Processing Systems (NeurIPS)*, 32, 2019. 3

628 Kaiming He, Xiangyu Zhang, Shaoqing Ren, and Jian Sun. Deep residual learning for image  
 629 recognition. In *IEEE Conference on Computer Vision and Pattern Recognition (CVPR)*, pp.  
 630 770–778, 2016. 7, 16

631

632 Zhengbao He, Tao Li, Xinwen Cheng, Zhehao Huang, and Xiaolin Huang. Towards natural machine  
 633 unlearning. *IEEE Transactions on Pattern Analysis and Machine Intelligence (TPAMI)*, 2025. 2

634

635 Tuan Hoang, Santu Rana, Sunil Gupta, and Svetha Venkatesh. Learn to unlearn for deep neural  
 636 networks: Minimizing unlearning interference with gradient projection. In *IEEE/CVF Winter  
 637 Conference on Applications of Computer Vision*, pp. 4819–4828, 2024. 3

638 Judy Hoffman, Daniel A Roberts, and Sho Yaida. Robust learning with jacobian regularization. *arXiv  
 639 preprint arXiv:1908.02729*, 2019. 24

640

641 James Kirkpatrick, Razvan Pascanu, Neil Rabinowitz, Joel Veness, Guillaume Desjardins, Andrei A  
 642 Rusu, Kieran Milan, John Quan, Tiago Ramalho, Agnieszka Grabska-Barwinska, et al. Overcoming  
 643 catastrophic forgetting in neural networks. *Proceedings of the national academy of sciences*, 114  
 644 (13):3521–3526, 2017. 9

645

646 Pang Wei Koh and Percy Liang. Understanding black-box predictions via influence functions. In  
 647 *International Conference on Machine Learning (ICML)*, pp. 1885–1894. PMLR, 2017. 2, 3

648

649 Alex Krizhevsky, Geoffrey Hinton, et al. Learning multiple layers of features from tiny images. 2009.  
 650 7, 16

648 Meghdad Kurmanji, Peter Triantafillou, Jamie Hayes, and Eleni Triantafillou. Towards unbounded  
 649 machine unlearning. *Advances in Neural Information Processing Systems (NeurIPS)*, 36, 2023. 1,  
 650 3, 7, 17, 23, 26

651

652 Ya Le and Xuan Yang. Tiny imagenet visual recognition challenge. *CS 231N*, 7(7):3, 2015. 7, 16

653

654 Shen Lin, Xiaoyu Zhang, Chenyang Chen, Xiaofeng Chen, and Willy Susilo. Erm-ktp: Knowledge-  
 655 level machine unlearning via knowledge transfer. In *Proceedings of the IEEE/CVF Conference on*  
 656 *Computer Vision and Pattern Recognition (CVPR)*, pp. 20147–20155, 2023. 3, 26

657

658 Jiancheng Liu, Parikshit Ram, Yuguang Yao, Gaowen Liu, Yang Liu, PRANAY SHARMA, Sijia Liu,  
 659 et al. Model sparsity can simplify machine unlearning. *Advances in Neural Information Processing*  
 660 *Systems (NeurIPS)*, 36, 2024. 3, 17, 26

661

662 Ronak Mehta, Sourav Pal, Vikas Singh, and Sathya N Ravi. Deep unlearning via randomized  
 663 conditionally independent hessians. In *IEEE/CVF Conference on Computer Vision and Pattern*  
 664 *Recognition (CVPR)*, pp. 10422–10431, 2022. 3

665

666 Xianjia Meng, Yong Yang, Ximeng Liu, and Nan Jiang. Active forgetting via influence estimation  
 667 for neural networks. *International Journal of Intelligent Systems*, 37(11):9080–9107, 2022. 3

668

669 Fan Mo, Anastasia Borovykh, Mohammad Malekzadeh, Soteris Demetriadis, Deniz Gündüz, and  
 670 Hamed Haddadi. Quantifying and localizing usable information leakage from neural network  
 671 gradients. *arXiv preprint arXiv:2105.13929*, 2021. 27

672

673 Seth Neel, Aaron Roth, and Saeed Sharifi-Malvajerdi. Descent-to-delete: Gradient-based methods  
 674 for machine unlearning. In *Algorithmic Learning Theory*, pp. 931–962. PMLR, 2021. 2, 26

675

676 Yuval Netzer, Tao Wang, Adam Coates, Alessandro Bissacco, Baolin Wu, Andrew Y Ng, et al.  
 677 Reading digits in natural images with unsupervised feature learning. In *NIPS workshop on deep*  
 678 *learning and unsupervised feature learning*, volume 2011, pp. 7. Granada, Spain, 2011. 7, 16

679

680 Vardan Petyan. Traces of class/cross-class structure pervade deep learning spectra. *Journal of*  
 681 *Machine Learning (JMLR)*, 21(1):10197–10260, 2020. 26

682

683 Vardan Petyan, XY Han, and David L Donoho. Prevalence of neural collapse during the terminal  
 684 phase of deep learning training. *Proceedings of the National Academy of Sciences (PNAS)*, 117  
 685 (40):24652–24663, 2020. 26

686

687 Alexandra Peste, Dan Alistarh, and Christoph H Lampert. SSSE: Efficiently erasing samples from  
 688 trained machine learning models. In *NeurIPS 2021 Workshop Privacy in Machine Learning*, 2021.  
 689 3

690

691 Garima Pruthi, Frederick Liu, Satyen Kale, and Mukund Sundararajan. Estimating training data  
 692 influence by tracing gradient descent. *Advances in Neural Information Processing Systems*  
 693 (NeurIPS), 33:19920–19930, 2020. 3

694

695 Deepak Ravikumar, Efstathia Souflieri, Abolfazl Hashemi, and Kaushik Roy. Unveiling privacy,  
 696 memorization, and input curvature links. In *International Conference on Machine Learning*,  
 697 (ICML), 2024. 27

698

699 General Data Protection Regulation. General data protection regulation (GDPR). *Intersoft Consulting*,  
 700 *Accessed in October*, 24(1), 2018. 1

701

702 Ramprasaath R Selvaraju, Michael Cogswell, Abhishek Das, Ramakrishna Vedantam, Devi Parikh,  
 703 and Dhruv Batra. Grad-cam: Visual explanations from deep networks via gradient-based lo-  
 704 calization. In *IEEE International Conference on Computer Vision (ICCV)*, pp. 618–626, 2017.  
 705 25

706

707 Thanveer Shaik, Xiaohui Tao, Haoran Xie, Lin Li, Xiaofeng Zhu, and Qing Li. Exploring the  
 708 landscape of machine unlearning: A survey and taxonomy. *arXiv preprint arXiv:2305.06360*, 1(2),  
 709 2023. 2

702 Reza Shokri, Marco Stronati, Congzheng Song, and Vitaly Shmatikov. Membership inference attacks  
 703 against machine learning models. In *2017 IEEE Symposium on Security and Privacy (SP)*, pp.  
 704 3–18. IEEE, 2017. 1

705 Daniel Smilkov, Nikhil Thorat, Been Kim, Fernanda Viégas, and Martin Wattenberg. Smoothgrad:  
 706 removing noise by adding noise. *arXiv preprint arXiv:1706.03825*, 2017. 25

708 Christoforos N Spartalis, Theodoros Semertzidis, Efstratios Gavves, and Petros Daras. Lotus: Large-  
 709 scale machine unlearning with a taste of uncertainty. In *Proceedings of the Computer Vision and*  
 710 *Pattern Recognition Conference*, pp. 10046–10055, 2025. 7, 17

711 Suraj Srinivas and François Fleuret. Rethinking the role of gradient-based attribution methods for  
 712 model interpretability. In *9th International Conference on Learning Representations (ICLR)*, 2021.  
 713 6

714 Vinith Suriyakumar and Ashia C Wilson. Algorithms that approximate data removal: New results  
 715 and limitations. *Advances in Neural Information Processing Systems (NeurIPS)*, pp. 18892–18903,  
 716 2022. 2

718 Ayush K Tarun, Vikram S Chundawat, Murari Mandal, and Mohan Kankanhalli. Fast yet effective  
 719 machine unlearning. *IEEE Transactions on Neural Networks and Learning Systems*, 2023. 3

720 Anvith Thudi, Gabriel Deza, Varun Chandrasekaran, and Nicolas Papernot. Unrolling sgd: Under-  
 721 standing factors influencing machine unlearning. In *2022 IEEE 7th European Symposium on*  
 722 *Security and Privacy (EuroS&P)*, pp. 303–319. IEEE, 2022. 1, 7, 17, 18, 26

723 Hanling Tian, Yuhang Liu, Mingzhen He, Zhengbao He, Zhehao Huang, Ruikai Yang, and Xiaolin  
 724 Huang. Simulating training dynamics to reconstruct training data from deep neural networks. In  
 725 *The Thirteenth International Conference on Learning Representations (ICLR)*, 2025. 1

727 Cheng-Long Wang, Qi Li, Zihang Xiang, and Di Wang. Has approximate machine unlearning been  
 728 evaluated properly? from auditing to side effects. *arXiv preprint arXiv:2403.12830*, 2024a. 9, 16

729 Weiqi Wang, Zhiyi Tian, and Shui Yu. Machine unlearning: A comprehensive survey. *arXiv preprint*  
 730 *arXiv:2405.07406*, 2024b. 1, 2, 10

731 Alexander Warnecke, Lukas Pirch, Christian Wressnegger, and Konrad Rieck. Machine unlearning  
 732 of features and labels. In *30th Annual Network and Distributed System Security Symposium, NDSS*,  
 733 2023. 7, 17

735 Ga Wu, Masoud Hashemi, and Christopher Srinivasa. Puma: Performance unchanged model  
 736 augmentation for training data removal. In *AAAI Conference on Artificial Intelligence (AAAI)*,  
 737 volume 36, pp. 8675–8682, 2022. 3

738 Jing Wu and Mehrtash Harandi. Munba: Machine unlearning via nash bargaining. In *Proceedings of*  
 739 *the IEEE/CVF International Conference on Computer Vision*, pp. 4754–4765, 2025. 7, 17

740 Yinjun Wu, Edgar Dobriban, and Susan Davidson. Deltagrad: Rapid retraining of machine learning  
 741 models. In *International Conference on Machine Learning (ICML)*, pp. 10355–10366. PMLR,  
 742 2020. 3, 26

743 Jie Xu, Zihan Wu, Cong Wang, and Xiaohua Jia. Machine unlearning: Solutions and challenges.  
 744 *IEEE Transactions on Emerging Topics in Computational Intelligence*, 8(3):2150–2168, 2024. 2,  
 745 7, 16

747 Bo Zhao, Konda Reddy Mopuri, and Hakan Bilen. idlg: Improved deep leakage from gradients.  
 748 *arXiv preprint arXiv:2001.02610*, 2020. 27

749 Kairan Zhao and Peter Triantafillou. Scalability of memorization-based machine unlearning. *arXiv*  
 750 *preprint arXiv:2410.16516*, 2024. 27

751 Kairan Zhao, Meghdad Kurmanji, George-Octavian Bărbulescu, Eleni Triantafillou, and Peter Tri-  
 752 antafillou. What makes unlearning hard and what to do about it. *Advances in Neural Information*  
 753 *Processing Systems*, 37:12293–12333, 2024. 17, 21, 22, 27, 28

755 Ligeng Zhu, Zhijian Liu, and Song Han. Deep leakage from gradients. *Advances in Neural*  
 756 *Information Processing Systems (NeurIPS)*, 32, 2019. 1, 27

## APPENDIX

## A ETHICS STATEMENT

This work studies machine unlearning (MU), motivated by the “right to be forgotten,” with the goal of enhancing user privacy and data protection. All experiments are conducted on publicly available datasets and standard benchmark models; no sensitive or personally identifiable information is used. While unlearning techniques could in principle be misused to manipulate model behavior, our focus is on strengthening trust and accountability in machine learning systems. We believe this work contributes positively to the development of privacy-preserving and ethically responsible AI.

## B REPRODUCIBILITY STATEMENT

We include anonymized supplementary materials containing the complete algorithm implementations for executing all experiments. We provide detailed experimental settings, hyperparameters, datasets, and evaluation metrics in our Appendix to ensure reproducibility.

## C THE USE OF LLMS

Large language models (LLMs) were employed solely as auxiliary writing tools. Their usage was strictly limited to surface-level assistance, including grammar correction, stylistic polishing, clarity improvement, and formatting consistency. LLMs were not involved in formulating research ideas, designing methods, conducting analyses, interpreting results, or drawing conclusions. At no stage were LLMs used to generate original content, experimental designs, or theoretical claims. All text segments refined with LLM assistance were subsequently reviewed, validated, and, where necessary, rewritten by the authors to ensure technical accuracy and precision of expression. The authors bear full responsibility for the final presentation and content of this paper. This disclosure is made in accordance with conference guidelines on LLM usage to ensure transparency and research integrity.

## D A TOY EXAMPLE COMPLEMENTING SAMPLE CONTRIBUTION DERIVATION

We use a simple MLP model to illustrate the insight of  $\mathcal{S}_k(\hat{x}, \tilde{x}) < \mathcal{S}_k(\hat{x}, \hat{x})$  with  $\hat{x} \neq \tilde{x}$ . Assume the  $l^{th}$  layer output of model is  $x^l = \phi(\theta^l x^{l-1})$ , where  $\theta^l$  refers to  $l^{th}$  layer parameter and  $\phi$  refers to activation function. Then,

$$g_k = \frac{\partial f_k}{\partial \theta^l} = \frac{\partial f_k}{\partial (\theta^l x^{l-1})} x^{l-1^T}, \quad (A1)$$

$$\begin{aligned} g'_k &= \frac{\partial f_k}{\partial \theta^l \partial x} = \frac{\partial f_k}{\partial (\theta^l x^{l-1})} \frac{\partial x^{l-1^T}}{\partial x} \\ &= \frac{\partial f_k}{\partial (\theta^l x^{l-1})} \phi'(\theta^{l-1} x^{l-2}) \theta^{l^T} \frac{\partial x^{l-2}}{\partial x}. \end{aligned} \quad (A2)$$

Thereby, the inner-dot  $g'_k(\hat{x})g_k(\tilde{x}) \propto \hat{x}^{l-1} \phi'(\theta^{l-1} \hat{x}^{l-2})$ . If ReLU activation is used, where  $\phi'(x) = 1$  if  $x > 0$  else  $\phi'(x) = 0$ ,  $\mathcal{S}_k(\hat{x}, \tilde{x}) \propto g'_k(\hat{x})g_k(\tilde{x})$  will be quite small. The conclusion here is that the residual term is relatively smaller than the contribution term. Therefore, the contribution of a training sample to the training process would be approximately reflected in the pre-trained model’s output sensitivity to the sample.

Additionally, we investigate sensitivity signatures across different samples (*i.e.*, different memorization levels and influence scores) in Appendix I.2. We find that highly memorized samples exhibit smaller sensitivity gap than low and middle memorized sample, and more influential samples exhibit higher sensitivity gap. This empirical evidence further confirms that our proposed sensitivity gap successfully reflect sample contribution and the residual term is not that crucial to some extent.

## 810 E STOPPING GUIDANCE 811

812 The optimization should cease once the withdrawal is completed, requiring a stopping guideline  
813 for practical use. We monitor both the optimization objective and unlearning metrics during mini-  
814 mizing the MU-Mis loss Eq.(3) in Figure A1, using the example of unlearning with ResNet-18 on  
815 fullclass-CIFAR100-rocket. In Figure A1, different colors represent different learning rates and the  
816 purple dashed line represents the accuracy of the retrained model. A consistent trend on accuracy  
817 change during unlearning is observed across different learning rates: as the optimization of MU-Mis  
818 loss progresses, the accuracy of the forgetting data (FA) gradually decreases, the accuracy of the  
819 remaining (RA) and test data (TA) first decrease slightly and then grow up with the recovery of  
820  $\|\nabla_x f_{c'}(x, w_p)\|_F$ .

821 Notably, when  $\|\nabla_x f_{c'}(x, w)\|_F$  re-  
822 covers close to the level of its initial  
823 value  $\|\nabla_x f_{c'}(x, w_p)\|_F$ , RA ap-  
824 proaches the retrained model across  
825 different learning rates. There exists a  
826 clear relationship between the unlearn-  
827 ing progress and model performance,  
828 allowing for effective unlearning by  
829 stopping the optimization timely. To  
830 this end, we introduce a stopping  
831 threshold ratio  $\delta$  to regulate the time  
832 of stopping. We record the minimal  
833 value of irrelevant class logit sensi-  
834 tivity as  $\epsilon$  and terminate unlearning  
835 process when  $\|\nabla_x f_{c'}(\mathcal{D}_f, w)\|_F > \epsilon$   
836 and  $\frac{\|\nabla_x f_{c'}(\mathcal{D}_f, w)\|_F}{\|\nabla_x f_{c'}(\mathcal{D}_f, w_p)\|_F} > \delta$ .

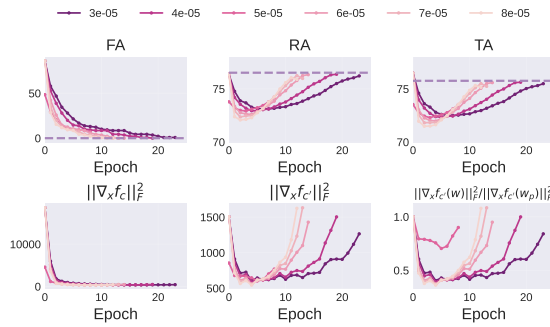
## 837 F EXPERIMENT DETAILS 838

### 839 F.1 EXPERIMENT SETTING 840

#### 841 Tasks, Datasets and Models.

842 We investigate 3 kinds of unlearning tasks in supervised image classification scenarios, including forgetting  
843 a full class, a sub-class under a super-class, and a random subset. We evaluate full class unlearning  
844 on CIFAR-100 (Krizhevsky et al., 2009), PinsFaceRecognition (Burak, 2020), and Tiny ImageNet  
845 (Le & Yang, 2015), sub-class unlearning on three sub-classes of CIFAR-20 (Krizhevsky et al., 2009),  
846 random subset unlearning on CIFAR-10 (Krizhevsky et al., 2009) and SVHN (Netzer et al., 2011).  
847 We perform sequential unlearning by iteratively unlearning a full and a sub-class to evaluate the  
848 algorithm’s robustness to privacy onion effect (Carlini et al., 2022). For iterative full class MU, we  
849 iteratively unlearn 5 distinct classes (label 0-4, corresponding to “Apple”, “Fish”, “Baby”, “Bear”  
850 and “Beaver”) of CIFAR-100 in line with Wang et al. (Wang et al., 2024a). For sub-class setting, we  
851 iteratively unlearn 5 sub-classes (“orchid”, “poppy”, “rose”, “sunflower”, “tulip”) under the same  
852 superclass “flower” of CIFAR-20. We use ResNet-18 (He et al., 2016) for all the above experiments.  
853 To further indicate the significant efficiency advantage of our remaining-data-free method, we perform  
854 full class unlearning on Tiny-ImageNet and sub-class unlearning on CIFAR-20 with ViT.

855 **Evaluation Metrics.** MU methods should be assessed from three aspects: *utility*, *privacy*, and  
856 *efficiency*(Xu et al., 2024). Beyond that, in practice, where the unlearning requests are made  
857 constantly, the unlearning *resilience* should be assessed, i.e. subsequent unlearning should not spoil  
858 previous unlearning efforts. For *utility*, we compute forgetting data accuracy (**FA**), remaining data  
859 accuracy (**RA**), and test data accuracy (**TA**) of the unlearned model. FA and RA are computed on the  
860 valid set in class-wise unlearning and on the train set in random subset unlearning. We compute the  
861 average gap (**Avg. Gap**) between the retrained model and the unlearned model on accuracy-related  
862 metrics, including FA, RA and TA to illustrate the utility disparity. In terms of *resilience*, we evaluate  
863 on sequential unlearning tasks. We compute the train (**FGTA**) and valid (**FGVA**) accuracy on the  
forgotten classes and quantify the unlearning resilience with the average of their disparity to the  
retrained model (**Resilience Avg. Gap**). To further examine the indistinguishability between the



849 Figure A1: Accuracy and optimization objective during  
850 fullclass-CIFAR100-rocket unlearning with different learn-  
851 ing rates on ResNet-18. FA decreases gradually, RA and  
852 TA first drop slightly and then rise with the recovery of  
853  $\|\nabla_x f_{c'}(x, w)\|_F$ . The endpoint of each curve corresponds  
854 to the time when  $\|\nabla_x f_{c'}\|_F$  exceeds 90% of its initial value.

864 retrained and unlearned model, we compute the **KL divergence** between their output distributions  
 865 over the entire dataset. The retrained model is an oracle of approximate MU, therefore, above disparity  
 866 metrics should be as small as possible. Regarding the *privacy* guarantee, we use membership inference  
 867 attack (**MIA**) (Chundawat et al., 2023) to probe the remaining information of the forgetting data. The  
 868 MIA success rate indicates how many samples in  $\mathcal{D}_f$  are predicted as membership samples of the  
 869 unlearned model. From a privacy perspective, a lower MIA value implies less information leakage  
 870 in the unlearned model and is preferred (Liu et al., 2024). For *efficiency*, we provide the run time  
 871 efficiency (**RTE**) in **seconds** to indicate timeliness.

872 **Baselines.** We compare our method along with 6 baselines which utilize the remaining data, as well  
 873 as 4 remaining-data-free methods. The 6 baselines include Bad Teacher (**BT**) (Chundawat et al.,  
 874 2023), Finetune (**FT**) (Warnecke et al., 2023), SCalable Remembering and Unlearning unBound  
 875 (**SCRUB**) (Kurmanji et al., 2023), Selective-Synaptic-Dampening (**SSD**) (Foster et al., 2024b),  
 876 Distance-based Unlearning via Centroid Kinematics (**DUCK**) (Cotogni et al., 2023), Saliency-based  
 877 unlearning (**SalUn**) (Fan et al., 2024b), Large-Scale Machine Unlearning with a Taste of Uncertainty  
 878 (**LoTUS**) (Spartalis et al., 2025), Machine Unlearning via Nash Bargaining (**MUNBa**) (Wu & Harandi,  
 879 2025). We also add a strong remaining-data-dependent method Refined-Unlearning Meta-algorithm  
 880 (**RUM**) (Zhao et al., 2024) for the most challenging random subset setting. The 4 remaining-data-free  
 881 methods include Random Labeling (**RL**) (Golatkar et al., 2020), Negative Gradient (**NG**) (Thudi  
 882 et al., 2022), Just in Time unlearning (**JiT**) (Foster et al., 2024a) and Selective-distillation for Class  
 883 and Architecture-agnostic unleaRning (**SCAR**) (Bonato et al., 2024).

884 The detailed method of each baseline is as the following:

- 885 • **BT** (Chundawat et al., 2023): Bad Teacher transfers knowledge from useful and useless  
 886 teachers for the remaining data and the forgetting data. The code source is <https://github.com/if-loops/selective-synaptic-dampening>.  
 887
- 888 • **FT** (Warnecke et al., 2023): Finetune optimizes the pre-trained model with the remaining  
 889 data, unlearning relying on “catastrohic forgetting”. The code source is <https://github.com/if-loops/selective-synaptic-dampening>.  
 890
- 891 • **SCRUB** (Kurmanji et al., 2023): SCRUB aims to push outputs of the student model (the  
 892 unlearned model) away from the teacher model (the pre-trained model) to distill knowledge.  
 893 This is achieved by first performing several max-steps (distill the knowledge) and then  
 894 perform several min-steps (regain performance on the remaining data with cross-entropy  
 895 loss). The code source is <https://github.com/meghdadk/SCRUB>.  
 896
- 897 • **SSD** (Foster et al., 2024b): SSD uses the Fisher information matrix to assess parameter  
 898 importance and suppress parameters that are important to the forgetting data while less im-  
 899 portant to the remaining data. The code source is <https://github.com/if-loops/selective-synaptic-dampening>.  
 900
- 901 • **DUCK** (Cotogni et al., 2023): DUCK employs metric learning to guide the removal of  
 902 samples matching the nearest incorrect centroid in the embedding space. The code source is  
 903 <https://github.com/OcraM17/DUCK>.  
 904
- 905 • **SalUn** (Fan et al., 2024b): SalUn computes weight saliency map to enable the most im-  
 906 portant weights for the forgetting data. The code source is <https://github.com/OPTML-Group/Unlearn-Saliency>.  
 907
- 908 • **LoTUS** (Spartalis et al., 2025): LoTUS performs large-scale machine unlearning by es-  
 909 timating and propagating uncertainty to guide parameter update suppression, enabling  
 910 scalable forgetting without relying on remaining data. The source code is <https://github.com/sohomghosh/LoTUS>.  
 911
- 912 • **MUNBa** (Wu & Harandi, 2025): MUNBa formulates machine unlearning as a Nash bar-  
 913 gaining problem and jointly optimizes forgetting and retention objectives to balance util-  
 914 ity preservation and effective removal. The source code is <https://github.com/OPTML-Group/MUNBa>.  
 915
- 916 • **RUM** (Zhao et al., 2024): RUM analyzes fundamental factors that impact unlearning  
 917 difficulty (e.g., embedding-space entanglement between forgotten and retained data, and

918 memorization levels), and proposes a meta-algorithm that partitions the forget set into  
 919 homogeneous subsets and applies per-subset unlearning to improve performance. The  
 920 source code is <https://github.com/kairanzhao/RUM>.  
 921

- **NG** (Thudi et al., 2022): Negative gradient computes several steps of gradient ascent with  
 922 the forgetting data. The source code is <https://github.com/jbonato1/scar>.
- **RL** (Golatkar et al., 2020): Random label relabels the forgetting data with randomly  
 924 assigned class and fine-tune the model with computed cross-entropy loss. The source code  
 925 is <https://github.com/jbonato1/scar>.
- **SCAR** (Bonato et al., 2024): SCAR utilizes Out-of-distribution (OOD) data as a surrogate for  
 927 the remaining data and distills the knowledge of the original model into the unlearned model  
 928 to preserve model utility. The source code is [https://github.com/jbonato1/  
 929 scar](https://github.com/jbonato1/scar).
- **JiT** (Foster et al., 2024a): JiT smooths the model output around the forgetting data by  
 931 minimizing the local Lipschitz constant. The source code is [https://github.com/  
 932 jwf40/Information-Theoretic-Unlearning](https://github.com/jwf40/Information-Theoretic-Unlearning).

## 934 F.2 KL DIVERGENCE

936 The KL divergence between two distributions is:

$$937 D_{\text{KL}}(p_z(w_r) \parallel p_z(w_u)) = \int p_z(w_r) \log[p_z(w_r)/p_z(\theta)] d\mathcal{D} \quad (A3)$$

939 We calculate empirical KL divergence with the entire dataset (including both the train and valid set).  
 940 We first collect the predicted class probabilities from both the unlearned and retrained models of each  
 941 sample, then we compute the output KL divergence as follows:

$$942 D_{\text{KL}} = \frac{1}{N} \sum_{i=1}^N \sum_{c=1}^C p_c(x_i; w_r) \log \frac{p_c(x_i; w_r)}{p_c(x_i; w_u)}, \quad (A4)$$

945 where  $N$  is total number of dataset,  $C$  denotes the total number of classes,  $w_u$  is the unlearned model  
 946 parameter and  $w_r$  is the retrained model parameter.  $p_c(x_i, w)$  represents the  $c$ -th posterior probability  
 947 of  $i$ -th sample in model  $w$ .

## 948 F.3 TRAINING DETAILS

950 For **ResNet-18**, training uses SGD with a momentum of 0.9, weight decay of  $5 \times 10^{-4}$ , and batch  
 951 size of 128 with a learning rate initialized at 0.1. The learning rate decays at 60,120,160 by 0.1 with  
 952 a total of 200 epochs.

953 For **ViT**, we initialize with model pre-trained on ImageNet provided by torchvision. Then we  
 954 randomly initialize the last fully connected layers and train it with SGD with a momentum of 0.9,  
 955 weight decay of  $5 \times 10^{-4}$ , batch size 64, constant learning rate  $\eta = 0.1$  for 10 epochs. All the  
 956 experiments are conducted on a single RTX 4090.

## 958 F.4 HYPER-PARAMETERS

960 For **MU-Mis**, we optimize the pretrained model under **model.eval()** mode with **vanilla SGD** without  
 961 momentum for ResNet-18 and Adam for ViT. For only the forgetting data are used in MU-Mis, we  
 962 must freeze the batch norm layers to avoid spoiling the remaining data. We use batch size of 256  
 963 for MU-Mis across all the experiments with ResNet-18 and batch size of 32 with ViT. We report the  
 964 learning rate  $\eta$  and stopping threshold  $\delta$  used in different settings in Table A4 for reproducibility.

965 For each baseline, We perform grid search to find the best hyper-parameters in each setting. The  
 966 hyper-parameter sweep range for each method is presented in Table A3. The hyper-parameters used  
 967 for all the methods in sequential full class and sub-class tasks are shown in Table A1 and Table A2.  
 968 For all the methods, we fix batch size as 256 for ResNet-18 and 64 for ViT unless otherwise stated in  
 969 hyper-parameter ranges. For BT, we use constant learning rate. For fine-tune based methods, e.g.  
 970 FT, as well as SCRUB and SalUn, we use cosine scheduler. We fix temperature= 1, alpha = 0.5,  
 971 gamma = 0.99, weight decay =  $5 \times 10^{-4}$  for SCRUB. We fix weight decay =  $5 \times 10^{-4}$  for DUCK  
 and SCAR.

972

973

Table A1: Hyperparameters for full class sequential unlearning in Fig. 5.

Methods	Hyperparameters
Retrain	epoch = 200, lr = 0.1, milestones = [60, 120, 160].
BT	epoch = 10, lr = $\{5, 5, 5, 1, 5\} \times 10^{-5}$ , temperature scalar = {3, 1, 1, 1, 5}.
FT	epoch = 10, lr = $10^{-1}$ for all iterations.
SSD	dampening constant $\lambda = \{1, 1, 1, 1, 0.1\}$ , selection weight $\alpha = \{95, 70, 50, 70, 80\}$ .
SalUn	epoch = 10, lr = $10^{-3}$ , threshold = 0.6 for all iterations.
MU-Mis	epoch = 50, lr = $\{2, 1, 1, 0.5, 0.8\} \times 10^{-4}$

981

982

983

Table A2: Hyperparameters for subclass sequential unlearning in Fig. 5.

Methods	Hyperparameters
Retrain	epoch = 200, lr = 0.1, milestones = [60, 120, 160].
BT	epoch = $\{5, 10, 5, 10, 5\}$ , lr = $\{0.5, 0.5, 1, 1, 5\} \times 10^{-5}$ , temperature scalar = {5, 5, 5, 3, 1}.
FT	epoch = 20, lr = $10^{-1}$ for all iterations.
SSD	dampening constant $\lambda = \{1, 0.1, 0.1, 1, 1\}$ , selection weight $\alpha = \{71, 100, 90, 87, 85\}$ .
SalUn	epoch = 10, lr = $10^{-3}$ , threshold = 0.6 for all iterations.
MU-Mis	epoch = 30, lr = $\{5, 1, 0.1, 3, 3\} \times 10^{-6}$ , stopping threshold $\delta = \{1.4, 1.4, 0.95, 10, 10\}$ .

991

992

993

Table A3: Hyper-parameters range overview for different methods in all the experiments.

Methods	Hyperparameters
BT	epoch $\in \{1, 3, 5, 10\}$ , lr $\in \{10^{-1}, 10^{-2}, 10^{-3}, 10^{-4}, 10^{-5}, 5 \times 10^{-5}, 5 \times 10^{-6}, 10^{-6}\}$ , temperature scalar $\in \{1, 3, 5\}$ .
FT	epoch $\in \{5, 10, 15, 20\}$ , lr $\in \{10^{-1}, 10^{-2}, 10^{-3}\}$ .
SSD	dampening constant $\lambda \in \{0.1, 0.5, 0.9, 1\}$ , selection weight $\alpha \in \{1, 5, 10, 20, 25, 30, 40, 50, 60, 70, 80, 90, 100\}$ .
SCRUB	epoch = 10, lr $\in \{10^{-1}, 5 \times 10^{-2}, 10^{-2}, 5 \times 10^{-3}, 10^{-3}, 5 \times 10^{-4}, 10^{-4}, 5 \times 10^{-5}, 10^{-5}\}$ , max step $\in \{2, 3, 5, 8\}$ .
SalUn	epoch $\in \{10, 20\}$ , lr $\in \{10^{-2}, 10^{-3}, 5 \times 10^{-4}, 5 \times 10^{-5}, 10^{-5}, 5 \times 10^{-6}, 10^{-6}\}$ , threshold $\in \{0.2, 0.3, 0.4, 0.5, 0.6, 0.7, 0.8, 0.9\}$ .
DUCK	lr $\in \{5 \times 10^{-2}, 10^{-2}, 5 \times 10^{-3}, 10^{-3}, 10^{-4}\}$ , $\lambda_1, \lambda_2 \in \{0.5, 1, 1.2, 1.5, 2, 3, 5\}$ .
NG	epoch $\in \{1, 3, 5, 10, 15, 20, 25, 30\}$ , lr $\in \{10^{-1}, 10^{-2}, 10^{-3}, 10^{-4}, 10^{-5}\}$ .
RL	epoch $\in \{1, 3, 5, 10, 15, 20, 25, 30\}$ , lr $\in \{10^{-1}, 10^{-2}, 10^{-3}, 10^{-4}, 10^{-5}\}$ .
JiT	dampening constant = 1, lr $\in [10^{-3}, 10^{-6}]$ , lipschitz weight $\alpha \in [0, 1]$ .
SCAR	lr $\in \{10^{-2}, 5 \times 10^{-3}, 10^{-3}, 5 \times 10^{-4}, 10^{-4}, 5 \times 10^{-5}, 5 \times 10^{-6}, 10^{-6}\}$ , batch size $\in \{256, 512, 1024\}$ , temperature $\in \{1, 3, 5\}$ , $\lambda_1, \lambda_2 \in \{1, 1.5, 3, 5\}$ .
LoTUS	lr $\in \{10^{-5}, 5 \times 10^{-5}, 10^{-4}, 5 \times 10^{-4}, 10^{-3}, 5 \times 10^{-3}, 10^{-2}, 5 \times 10^{-2}, 10^{-1}\}$ , epochs $\in \{5, 10, 15, 20\}$ , $\alpha \in \{2, 4, 6, 8, 16\}$ .
MUNBa	lr $\in \{10^{-5}, 5 \times 10^{-5}, 10^{-4}, 5 \times 10^{-4}, 10^{-3}, 5 \times 10^{-3}, 10^{-2}, 5 \times 10^{-2}, 10^{-1}\}$ , epochs $\in \{5, 10, 15, 20, 25, 30, 40\}$ .

1025

1026  
 1027  
 1028  
 1029  
 1030  
 1031  
 1032  
 1033  
 1034  
 1035  
 1036  
 1037  
 1038  
 1039  
 1040  
 1041  
 1042  
 1043  
 1044  
 1045  
 1046  
 1047

1048 Table A4: Hyperparameters of MU-Mis h(learning rate  $\eta$  and stopping threshold ratio  $\delta$ ).  
 1049

Setting	$\eta$	$\delta$
fullclass-CIFAR-100	$7 \times 10^{-5}$	1.45
fullclass-PinsFaceRecognition	$4 \times 10^{-4}$	0.68
fullclass-Tiny-ImageNet	$4 \times 10^{-6}$	1.1
subclass-CIFAR-20-rocket	$3 \times 10^{-5}$	3.00
subclass-CIFAR-20-sea	$2 \times 10^{-5}$	0.93
subclass-CIFAR-20-lamp	$5 \times 10^{-5}$	1.80
fullclass-Tiny-ImageNet-ViT	$5 \times 10^{-4}$	1.03

1050  
 1051  
 1052  
 1053  
 1054  
 1055  
 1056  
 1057  
 1058  
 1059  
 1060  
 1061  
 1062  
 1063  
 1064  
 1065  
 1066  
 1067  
 1068  
 1069  
 1070  
 1071  
 1072  
 1073  
 1074  
 1075  
 1076  
 1077  
 1078  
 1079

## 1080 G ADDITIONAL EXPERIMENT RESULTS

### 1081 G.1 UNLEARNING UTILITY

#### 1082 G.1.1 FULL CLASS MU ON PINSFACERECOGNITION

1083 Results of full class unlearning on PinsFaceRecognition dataset are presented in Table A5. MU-Mis  
 1084 exhibits the smallest Avg.Gap to the retrained model, alongside a low MIA susceptibility. SCRUB  
 1085 and Salun exhibit a notably high MIA score, demonstrating a high risk of privacy leakage.

1086 Table A5: Performance overview for **full class** unlearning (including MU-Mis and 6 baselines)  
 1087 evaluated on PinsFaceRecognition with ResNet-18. The content format follows Table 1.

Method	RA	FA	TA	Avg. Gap ↓	MIA	RTE
Pretrain	93.49	100	93.59	34.54	100.00	13144
Retrain	93.06 <sub>±0.21</sub>	0.00 <sub>±0.00</sub>	92.25 <sub>±0.32</sub>	0.00	0.00 <sub>±0.00</sub>	11400
BT	92.69 <sub>±0.01</sub>	0.00 <sub>±0.00</sub>	91.48 <sub>±0.01</sub>	0.26	0.00 <sub>±0.00</sub>	36
FT	93.99 <sub>±0.09</sub>	8.78 <sub>±1.34</sub>	92.94 <sub>±0.10</sub>	3.47	0.00 <sub>±0.00</sub>	146
SCRUB	92.82 <sub>±0.02</sub>	0.00 <sub>±0.00</sub>	91.61 <sub>±0.02</sub>	0.29	19.63 <sub>±0.28</sub>	112
SSD	93.41 <sub>±0.00</sub>	0.00 <sub>±0.00</sub>	92.17 <sub>±0.00</sub>	0.14	0.00 <sub>±0.00</sub>	8
DUCK	92.17 <sub>±0.11</sub>	0.00 <sub>±0.00</sub>	91.06 <sub>±0.11</sub>	0.69	0.00 <sub>±0.00</sub>	64
SalUn	93.28 <sub>±0.05</sub>	0.62 <sub>±0.00</sub>	92.12 <sub>±0.06</sub>	0.34	54.22 <sub>±1.06</sub>	154
MunBa	91.44 <sub>±0.12</sub>	1.63 <sub>±0.02</sub>	90.27 <sub>±0.11</sub>	1.74	0.00 <sub>±0.00</sub>	522
LoTus	92.87 <sub>±0.08</sub>	0.00 <sub>±0.00</sub>	91.75 <sub>±0.09</sub>	0.23	0.00 <sub>±0.00</sub>	374
MU-Mis	92.98 <sub>±0.06</sub>	0.00 <sub>±0.00</sub>	92.13 <sub>±0.04</sub>	0.07	0.00 <sub>±0.00</sub>	24

#### 1103 G.1.2 SUB CLASS MU ON CIFAR-20-LAMP

1104 We evaluate sub-class unlearning on CIFAR-20-Lamp as presented in Table A6. The FA of the  
 1105 retrained model is 11.31, indicating certain generalization capability on the unlearned class. MU-Mis  
 1106 exhibits the smallest Avg.Gap to the retrained model.

1107 Table A6: Performance overview for **sub-class** unlearning (including proposed MU-Mis and 6  
 1108 baselines) evaluated on lamp of CIFAR-20 using ResNet-18. The content format follows Table 1.

Method	RA	FA	TA	Avg. Gap ↓	MIA	RTE
Pretrain	85.31	74.22	85.21	21.30	92.82	6910
Retrain	85.12 <sub>±0.22</sub>	11.31 <sub>±1.60</sub>	84.40 <sub>±0.20</sub>	0.00	7.06 <sub>±0.11</sub>	4298
BT	85.52 <sub>±0.04</sub>	10.00 <sub>±0.00</sub>	84.84 <sub>±0.04</sub>	0.72	0.00 <sub>±0.00</sub>	29
FT	82.47 <sub>±0.15</sub>	14.00 <sub>±2.19</sub>	81.90 <sub>±0.18</sub>	1.97	2.80 <sub>±0.36</sub>	128
SCRUB	82.17 <sub>±0.68</sub>	19.00 <sub>±4.74</sub>	81.60 <sub>±0.70</sub>	4.48	26.20 <sub>±4.18</sub>	113
SSD	84.56 <sub>±0.00</sub>	15.00 <sub>±0.00</sub>	83.84 <sub>±0.00</sub>	1.60	0.60 <sub>±0.00</sub>	18
DUCK	83.25 <sub>±0.31</sub>	31.02 <sub>±2.74</sub>	82.69 <sub>±0.34</sub>	7.75	27.68 <sub>±5.15</sub>	68
SalUn	84.44 <sub>±0.05</sub>	13.70 <sub>±1.66</sub>	83.74 <sub>±0.04</sub>	1.24	1.68 <sub>±0.17</sub>	1007
MunBa	81.17 <sub>±0.15</sub>	17.00 <sub>±0.10</sub>	80.69 <sub>±0.14</sub>	4.45	5.00 <sub>±0.12</sub>	676
LoTus	27.44 <sub>±0.22</sub>	12.00 <sub>±0.08</sub>	27.40 <sub>±0.20</sub>	38.45	33.60 <sub>±0.18</sub>	14
MU-Mis	84.36 <sub>±0.51</sub>	11.70 <sub>±1.29</sub>	83.66 <sub>±0.50</sub>	0.63	0.00 <sub>±0.00</sub>	10

#### 1121 G.1.3 RANDOM SUBSET UNLEARNING

1122 We evaluate random subset unlearning on CIFAR-10 and SVHN as presented in Table A6. We could  
 1123 see that it is much more challenging for remaining-data-free methods to preserve model utility in this  
 1124 setting, for forgetting and remaining data are highly entangled in this scenario. Across CIFAR-10 and  
 1125 SVHN, MU-Mis exhibits consistently low MIA value, demonstrating a good privacy preservation.

1126 **Comparison with RUM in random subset setting.** RUM(Zhao et al., 2024) provides a careful  
 1127 analysis of what makes unlearning hard and applies tailored unlearning strategies to each group of  
 1128 homogeneous subsets (i.e., by memorization level), achieving excellent performance in especially  
 1129 challenging random-subset setting. Therefore, we follow the experiment of RUM (*i.e.*, Table 1 in its  
 1130 original paper, where random subset is consist of 3000 samples of high, middle, low memorization  
 1131 levels in CIFAR-10.) We compare performances of RUM, SalUn and MU-Mis in the following Table  
 1132 A8. We could see that MU-Mis still outperforms GA, but there is a clear performance gap between  
 1133 MU-Mis and RUM, indicating a room for further improvement.

1134 Table A7: Performance overview for **random subset (10%)** unlearning task evaluated on forgetting  
 1135 10% CIFAR-10 and SVHN using ResNet-18. The content format follows Table 1.

1136

Method	CIFAR-10						SVHN					
	RA	FA	TA	Avg. Gap↓	MIA	RTE	RA	FA	TA	Avg. Gap↓	MIA	RTE
Pretrain	100.00	99.96	94.68	1.84	92.64	14322	100.00	100.00	96.48	1.65	83.11	16904
Retrain	100.00 <sub>±0.00</sub>	94.51 <sub>±0.16</sub>	94.75 <sub>±0.11</sub>	0.00	84.77 <sub>±11.13</sub>	12800	100.00 <sub>±0.00</sub>	95.12 <sub>±0.12</sub>	96.40 <sub>±0.14</sub>	0.00	81.24 <sub>±11.13</sub>	13890
BT	99.64 <sub>±0.01</sub>	93.06 <sub>±0.06</sub>	93.01 <sub>±0.04</sub>	1.18	7.20 <sub>±0.00</sub>	50	98.73 <sub>±0.01</sub>	96.71 <sub>±0.03</sub>	95.01 <sub>±0.01</sub>	1.42	22.32 <sub>±0.00</sub>	215
FT	100.0 <sub>±0.00</sub>	94.73 <sub>±0.13</sub>	93.17 <sub>±0.25</sub>	0.51	68.66 <sub>±0.00</sub>	395	100.0 <sub>±0.00</sub>	96.38 <sub>±0.03</sub>	96.87 <sub>±0.09</sub>	0.54	80.72 <sub>±0.54</sub>	805
SCRUB	100.00 <sub>±0.00</sub>	95.79 <sub>±0.50</sub>	93.43 <sub>±0.10</sub>	0.87	77.56 <sub>±0.93</sub>	207	95.40 <sub>±1.18</sub>	94.79 <sub>±1.00</sub>	94.94 <sub>±0.83</sub>	1.98	23.15 <sub>±2.62</sub>	104
SSD	99.99 <sub>±0.00</sub>	99.98 <sub>±0.02</sub>	94.66 <sub>±0.01</sub>	1.86	92.54 <sub>±0.43</sub>	18	98.67 <sub>±0.39</sub>	98.63 <sub>±0.43</sub>	96.59 <sub>±0.11</sub>	1.52	84.23 <sub>±0.77</sub>	55
DUCK	98.04 <sub>±0.05</sub>	97.90 <sub>±0.21</sub>	92.38 <sub>±0.06</sub>	2.57	90.59 <sub>±0.29</sub>	21	96.16 <sub>±0.20</sub>	94.86 <sub>±0.39</sub>	95.53 <sub>±0.25</sub>	1.51	30.46 <sub>±0.28</sub>	156
SalUn	100.0 <sub>±0.00</sub>	94.31 <sub>±0.03</sub>	93.19 <sub>±0.03</sub>	0.59	26.52 <sub>±0.00</sub>	247	99.77 <sub>±0.00</sub>	94.50 <sub>±0.05</sub>	95.85 <sub>±0.01</sub>	0.47	19.92 <sub>±0.00</sub>	409
MunBu	100.00 <sub>±0.00</sub>	94.57 <sub>±0.10</sub>	93.19 <sub>±0.08</sub>	0.54	58.20 <sub>±0.18</sub>	420	99.73 <sub>±0.05</sub>	96.46 <sub>±0.06</sub>	96.84 <sub>±0.05</sub>	0.68	66.70 <sub>±0.20</sub>	583
LoTus	96.90 <sub>±0.12</sub>	96.73 <sub>±0.08</sub>	90.55 <sub>±0.11</sub>	3.17	56.10 <sub>±0.19</sub>	172	94.48 <sub>±0.14</sub>	94.31 <sub>±0.10</sub>	86.65 <sub>±0.13</sub>	5.36	78.80 <sub>±0.15</sub>	35
NG	96.46 <sub>±0.23</sub>	96.15 <sub>±0.35</sub>	90.52 <sub>±0.22</sub>	3.13	88.21 <sub>±0.32</sub>	25	98.98 <sub>±0.02</sub>	98.98 <sub>±0.05</sub>	96.56 <sub>±0.01</sub>	1.53	84.53 <sub>±0.26</sub>	25
RL	96.17 <sub>±0.28</sub>	93.99 <sub>±0.51</sub>	88.29 <sub>±0.34</sub>	4.27	83.11 <sub>±0.50</sub>	26	98.66 <sub>±0.05</sub>	98.53 <sub>±0.10</sub>	96.02 <sub>±0.02</sub>	1.56	73.94 <sub>±0.28</sub>	25
JIT	95.45 <sub>±1.92</sub>	95.46 <sub>±1.81</sub>	89.63 <sub>±1.90</sub>	3.54	86.00 <sub>±0.32</sub>	255	96.30 <sub>±0.64</sub>	96.26 <sub>±0.74</sub>	95.14 <sub>±0.89</sub>	1.88	62.78 <sub>±4.32</sub>	333
SCAR	98.63 <sub>±0.13</sub>	98.64 <sub>±0.08</sub>	92.43 <sub>±0.13</sub>	2.61	48.36 <sub>±0.35</sub>	197	96.34 <sub>±0.54</sub>	96.46 <sub>±0.69</sub>	92.39 <sub>±0.70</sub>	2.86	55.20 <sub>±2.86</sub>	158
MU-Mis	97.76 <sub>±0.03</sub>	97.43 <sub>±0.04</sub>	91.50 <sub>±0.03</sub>	2.80	33.04 <sub>±0.28</sub>	116	95.48 <sub>±0.00</sub>	95.50 <sub>±0.03</sub>	94.22 <sub>±0.00</sub>	2.36	26.11 <sub>±0.00</sub>	116

1147

1148 **The complementary roles of RUM, SalUn, and MU-Mis.** Nonetheless, it is worth noting that  
 1149 RUM, SalUn, and our MU-MIS focus on different aspects: **RUM** answers **how samples** (low →  
 1150 middle → high memorization) should be scheduled and treated during unlearning, **SalUn** identifies  
 1151 which parameters (gradient-based saliency map) should be updated, and **MU-Mis** figures out **what**  
 1152 **information** (sample contribution) should be removed. The three aspects are all important and  
 1153 numerically has their own advantages, e.g., RUM is perfect in random subset unlearning and MU-Mis  
 1154 work well without using remaining data. Therefore, RUM, SalUn and MU-Mis are not competing  
 1155 in the same design space, and are naturally complementary and can be combined. And we are very  
 1156 happy to see performance of RUM and especially the combination of RUM and MU-Mis. Combining  
 1157 RUM could improve performance of MU-Mis to some extent, but it still under-perform RUM by a  
 1158 noticeable margin on model utility.

1159 **MU-Mis exhibit lowest KL-divergence on forget set to the retrain model than SalUn and RUM.**  
 1160 Furthermore, we examine the KL divergence between MU-Mis and retrained model in Table A8.  
 1161 Surprisingly, we find that MU-Mis achieves the smallest KL-divergence to the retrain model in  
 1162 forget set across different methods. We attribute this to their fundamentally different unlearning  
 1163 mechanisms: RUM (inherited from fine-tuning and SalUn) relies on random relabeling or catastrophic  
 1164 forgetting. As discussed in our paper, random relabeling might not provide a principled way to  
 1165 align the output distribution of the retrain model on forgetting data, leading to a sub-optimal output  
 1166 distribution. Also, compared with RL, MU-Mis does improve existing RDF method in random subset  
 1167 unlearning. The overall KL divergence of RL is 4.3, while that of MU-Mis is 0.65, which is an  
 1168 substantial improvement, indicating that MU-Mis produces an output distribution much closer than  
 1169 other RDF methods. Consequently, although MU-Mis still underperforms remaining-data-dependent  
 1170 methods such as RUM+SalUn in terms of model utility, we think its lower KL divergence on the  
 1171 forgetting data is a meaningful step that advances unlearning towards a more faithful/reasonable  
 1172 unlearning.

1173 **Challenges of remainig-data-free methods in random subset removal.** As is investigated in Figure  
 1174 A4 in Appendix H, we could see that intra-class samples assemble highly similar gradients. Moreover,  
 1175 many existing remaining-data-dependent approaches are still suffering from utility degradation in  
 1176 this setting. Therefore, it is important to acknowledge the daunting challenges such a vision of  
 1177 remaining-data-free method in random subset setting faces. Although not perfect, but MU-Mis has  
 1178 advanced remaining-data-free method in this challenging scenario. Therefore, we remain hopeful  
 1179 about the vision of a perfectly RDF method that preserves model utility under random subset settings  
 1180 and we believe a better location of sample contribution might offer a promising path.

1180

1181 Table A8: Unlearning performance and KL divergence metrics of SalUn, RUM and MU-Mis on  
 1182 CIFAR-10 with ResNet-18 following Zhao et al. (2024).

1183

Method	FA	RA	TA	Avg. Gap↓	ToW	MIA	MIA.GAP	ToW_MIA	KL_Forget	KL_Test	KL_Retain	KL_All
Pretrain	100.00	100.00 <sub>±0.00</sub>	85.10 <sub>±0.12</sub>	12.24	0.64	0.03	0.45	0.44	2.7131	0.3040	0.0018	0.1826
Retrain	63.93 <sub>±0.15</sub>	100.00 <sub>±0.00</sub>	84.45 <sub>±0.11</sub>	0.00	1.00 <sub>±0.07</sub>	0.47 <sub>±0.05</sub>	0.00	1.00 <sub>±0.08</sub>	0.0000	0.0000	0.0000	0.0000
SalUn	73.63 <sub>±0.21</sub>	99.99 <sub>±0.01</sub>	81.64 <sub>±0.18</sub>	4.17	0.88 <sub>±0.06</sub>	0.79 <sub>±0.04</sub>	0.31	0.64 <sub>±0.07</sub>	0.9941	0.3601	0.0548	0.1175
RUM	66.40 <sub>±0.14</sub>	100.00 <sub>±0.00</sub>	84.41 <sub>±0.13</sub>	0.84	0.97 <sub>±0.05</sub>	0.99 <sub>±0.03</sub>	0.52	0.48 <sub>±0.09</sub>	1.4462	0.2770	0.0057	0.0675
RL	58.40 <sub>±0.24</sub>	62.32 <sub>±0.20</sub>	47.81 <sub>±0.15</sub>	26.62	0.37 <sub>±0.04</sub>	0.49 <sub>±0.08</sub>	0.02	0.34 <sub>±0.06</sub>	5.9854	4.5657	4.1801	4.3005
MU-Mis	66.90 <sub>±0.19</sub>	70.48 <sub>±0.22</sub>	57.37 <sub>±0.16</sub>	19.85	0.50 <sub>±0.03</sub>	0.42 <sub>±0.06</sub>	0.06	0.40 <sub>±0.04</sub>	<b>0.6525</b>	1.1091	1.2391	0.7509
RUM+MU-Mis	60.70 <sub>±0.23</sub>	77.45 <sub>±0.19</sub>	61.18 <sub>±0.14</sub>	16.35	0.58 <sub>±0.08</sub>	0.41 <sub>±0.07</sub>	0.06	0.56 <sub>±0.05</sub>	2.7765	1.0060	0.6421	0.7005

1188  
1189

## G.1.4 FULL CLASS MU COMPARED WITH JIT WITH VGG16

JiT unlearns by regularizing lipshitz constant around the forgetting data, which might fail on DNNs with batch norm layers. Following the architecture used in the original paper, we compare with it on CIFAR-100-rocket unlearning in Table A9. The results show that JiT exhibits greater efficacy when implemented with VGG-16 as opposed to ResNet-18. However, it still exhibits a noticeable performance disparity when compared to MU-Mis.

1199

1200  
1201

## G.1.5 SUB-CLASS MU ON CIFAR-20-SEA WITH ViT

1202  
1203  
1204  
1205

We conducted experiments with ViT on subclass-CIFAR20-sea to further demonstrate our effectiveness across different tasks. MU-Mis exhibits the best RA, FA, and TA, and provides advantages in unlearning time.

1206  
1207  
1208

Table A10: Performance overview for **sub-class** unlearning task evaluated on **Cifar20-Sea** using **ViT**. RTE is reported in **minute**.

Methods	RA	FA	TA	Avg. Gap ↓	MIA	RTE (min)
Pretrain	93.65	91.32	93.63	0.93	69.80	-
Retrain	93.90 <sub>±0.12</sub>	88.98 <sub>±0.08</sub>	93.84 <sub>±0.14</sub>	0.00	59.00 <sub>±0.23</sub>	-
SalUn	94.15 <sub>±0.10</sub>	89.29 <sub>±0.03</sub>	94.13 <sub>±0.08</sub>	0.27	62.10 <sub>±0.42</sub>	10
MU-Mis	93.70 <sub>±0.02</sub>	88.84 <sub>±0.25</sub>	93.67 <sub>±0.02</sub>	<b>0.17</b>	69.67 <sub>±0.31</sub>	0.5

1213  
1214

## G.2 MEMBERSHIP INFERENCE ATTACK

1215  
1216  
1217  
1218  
1219  
1220  
1221

We examine our privacy leakage with a comparably good unlearning-adapted LiRA proposed by SCRUB Kurmanji et al. (2023). We report SCRUB-LiRA examined results across 3 unlearning settings in Table A11. We could see that in MU-Mis unlearned model, SCRUB-LiRA is quite close to random guessing, indicating that the forgetting data in MU-Mis unlearned model is similar to non-members.

1222  
1223  
1224  
1225  
1226  
1227  
1228  
1229  
1230  
1231  
1232

**LiRA-SCRUB and MIA-Entropy is complementary.** The goal of the adversary in LiRA-based MIA is to distinguish “forgotten samples” from unseen (non-member) samples. Therefore, their criteria of successful unlearning is that in the unlearned model, the adversary could not well distinguish forgotten samples from unseen samples, i.e., MIA collapse to random guessing (50%) for random subset unlearning. LiRA-based MIA examines how indistinguishable the forgetting data to the non-members, thereby the closer of SCRUB-MIA value to 50% in random subset setting is the better. While MIA in our paper examines how much forgotten samples are predicted as members, thereby the lower is the better. That is to say, **LiRA-based MIA** examines the extent of **non-membership** of forgetting data, while our **MIA-Entropy** examines the extent of membership, i.e., the residual **membership** signals of forgetting data. Therefore, these 2 MIAs are not contradictory or competing, but complementary, which all support our conclusions.

1233  
1234

Table A11: SCRUB-LiRA scores across different unlearning settings.

Setting	Model	FA (%)	RA (%)	TA (%)	MIA-Entropy	MIA-SCRUB
Fullclass-CIFAR100-Rocket	Pretrain	86.00	76.37	76.56	95.40	73.40 <sub>±2.60</sub>
	Retrain	0.00	76.86	76.07	6.60	96.40 <sub>±1.60</sub>
	MU-Mis	0.00	76.37	75.71	0.00	90.40 <sub>±2.00</sub>
Subclass-CIFAR20-Sea	Pretrain	97.00	85.10	85.14	91.80	64.40 <sub>±2.40</sub>
	Retrain	80.00	84.85	85.00	53.00	47.40 <sub>±6.40</sub>
	MU-Mis	80.00	84.26	84.15	0.60	53.00 <sub>±4.60</sub>
Random-CIFAR10-10%	Pretrain	99.96	100.00	94.68	92.64	56.64 <sub>±0.60</sub>
	Retrain	94.51	100.00	94.75	84.77	49.68 <sub>±0.30</sub>
	MU-Mis	97.43	97.42	91.50	83.34	52.66 <sub>±0.40</sub>

1242 G.3 ABLATION STUDY  
12431244 G.3.1 ABLATION STUDY ON EACH TERM OF MU-MIS  
1245

1246 We study the role of each term in  
1247 our loss through ablation, illustrating  
1248 with fullclass-CIFAR100-Rocket on  
1249 ResNet-18. We denote the first term  
1250  $\|\nabla_x f_c(w, x)\|_F^2$  in our loss Eq. (3) as  
1251 TC (Target Class) and the second term  
1252  $\|\nabla_x f_{c'}(w, x)\|_F^2$  as OC (Other Class).  
1253 In Table A12, we showcase the un-  
1254 learning performance of decreasing  
1255 TC, increasing OC, and decreasing  
1256 TC - OC (MU-Mis) respectively. We also investigate another variant of MU-Mis: regressing  
1257 sensitivity norm of TC(target class) term to OC(other class) term. During unlearning, we observe  
1258 that as  $\|\nabla_x f_c\|_F$  decreases, FA decreases gradually. We find that although the gradient of  $\|\nabla_x f_{c'}\|_F$   
1259 is detached, its norm exhibits slight decrease as well when minimizing. As the sensitivity norm  
1260 of  $f_c$  approaches  $f_{c'}$ , i.e., the loss approaches 0, FA gradually stops to decrease and converges at  
1261 17.35%. Therefore, this variant could unlearn successfully but failed to preserve model utility by  
1262 regressing sensitivity magnitude of  $f_c$  to  $f_{c'}$ . As demonstrated by Figure A1, when minimizing  
1263  $\|\nabla_x f_c\|_F$ ,  $\|\nabla_x f_{c'}\|_F$  and retain accuracy (RA) will drop slightly as well, then RA will recover to  
1264 its original level as the picking up of  $\|\nabla_x f_{c'}\|_F$  in our loss. Therefore, the magnitude of  $\|\nabla_x f_{c'}\|_F$   
1265 is essential for preserving model utility on remaining data (which is also supported by the ablation  
1266 study in our Table A10). Thus, when regressing  $\|\nabla_x f_c\|_F$  to  $\|\nabla_x f_{c'}\|_F$ , the norm of  $\|\nabla_x f_{c'}\|_F$   
1267 is not explicitly preserved, and drops during minimizing. Therefore, this regressing variant is a useful  
1268 diagnose and it confirms that the joint-term optimization in MU-Mis is necessary.

1269 From the ablation study, we know that minimizing the first term obviates information of the  
1270 forgetting data, but greatly hurts performance on the remaining data. Solely increasing OC brings a  
1271 slight accuracy drop on remaining data, but hardly unlearns the forgetting data. While our MU-Mis  
1272 loss could unlearn effectively meanwhile preserve model utility on the remaining data.

## 1273 G.3.2 PERFORMANCE UNDER SENSITIVITY REGULARIZATION TECHNIQUE

1274 We employed Jacobian regularization Hoffman et al. (2019) to our pre-training and re-training.  
1275 Jacobian regularization penalizes model's input-output sensitivity around training sample  $x$ , i.e.,  
1276  $\|J(x)\| = \|\frac{\partial f(x)}{\partial x}\|_F$  to encourage a smoother decision boundary for better robustness and general-  
1277 ization. We evaluated the unlearning of an full class on the CIFAR-10 dataset by training ResNet18  
1278 for 30 epochs with lr = 0.1, bs = 256, regularization coefficient = 0.01. The unlearning performance is  
1279 shown in Table A14, where the first 3 rows are performances on vanilla model (with data augmentation  
1280 but without Jacobian regularization). In Jacobian regularized model, it seems to be more difficult  
1281 to fully forget a class by MU-Mis, but it still preserves model utility well without remaining data.

1282 G.3.3 ROBUSTNESS OF PERFORMANCE TO SENSITIVITY METRIC.  
1283

1284 We investigate performances of MU-  
1285 Mis with different sensitivity norm  
1286 choices in Table A13. We can see  
1287 that the  $L_2$  norm yields similar perfor-  
1288 mance to the Frobenius norm (origi-  
1289 nal MU-Mis) and retrain, suggesting  
1290 that the method is robust as long as  
1291 the norm aggregates all components  
1292 of the sensitivity vector. In contrast,  
1293 norms that emphasize only extreme  
1294 coordinates (e.g., infinity norm) tend to over-penalize the worst-case direction, which empirically  
1295 hurts model utility. We observed that the model tends to break down even under a very small learning  
1296 rate (1e-8) for  $L_1$  norm, which we attribute this to its non-smooth optimization, which induces abrupt  
1297 and sparse updates in model outputs.

1246 Table A12: Ablation study on each term of our loss in full  
1247 class (Rocket) unlearning. TC (Target Class) refers to the  
1248 first term and OC (Other Class) refers to the second term.

Methods	RA	FA	TA	Avg. Gap ↓	MIA	RTE
Pretrain	76.41	79.69	76.47	26.84	95.80	-
Retrain	$76.52 \pm 0.27$	$0.00 \pm 0.00$	$75.76 \pm 0.24$	0.00	$2.87 \pm 0.46$	-
TC	$65.41 \pm 0.00$	$0.00 \pm 0.00$	$64.73 \pm 0.00$	$7.38$	$1.40 \pm 0.00$	44
OC	$70.13 \pm 0.41$	$74.62 \pm 1.56$	$70.21 \pm 0.42$	$28.85$	$0.00 \pm 0.00$	25
TC-OC.detach()	$70.24 \pm 0.01$	$17.35 \pm 0.04$	$69.45 \pm 0.03$	9.98	$0.016 \pm 0.045$	
TC - OC	$76.42 \pm 0.07$	$0.00 \pm 0.00$	$75.64 \pm 0.07$	$0.07$	$0.00 \pm 0.00$	30

1246 Table A13: Performances of MU-Mis under different sensi-  
1247 tivity norm choices.

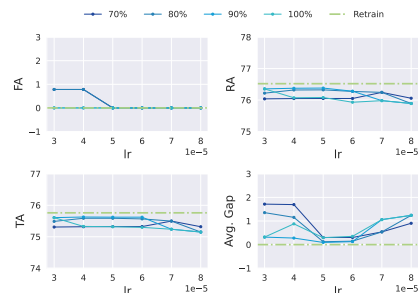
Methods	RA	FA	TA	Avg. Gap ↓	MIA
Pretrain	76.41	79.69	76.47	26.84	95.80
Retrain	$76.52 \pm 0.27$	$0.00 \pm 0.00$	$75.76 \pm 0.24$	0.00	$2.87 \pm 0.46$
$L_2$	$75.53 \pm 0.05$	$1.95 \pm 0.02$	$74.89 \pm 0.11$	1.27	$0.000 \pm 0.00$
Inf	$50.34 \pm 0.12$	$1.95 \pm 0.04$	$50.11 \pm 0.14$	17.93	$0.710 \pm 0.02$
Frobenius	$76.42 \pm 0.07$	$0.00 \pm 0.00$	$75.64 \pm 0.07$	$0.07$	$0.000 \pm 0.00$

1296 Table A14: Unlearning performance w/o Jacobian regularization on CIFAR-100-full-class-rocket.  
1297

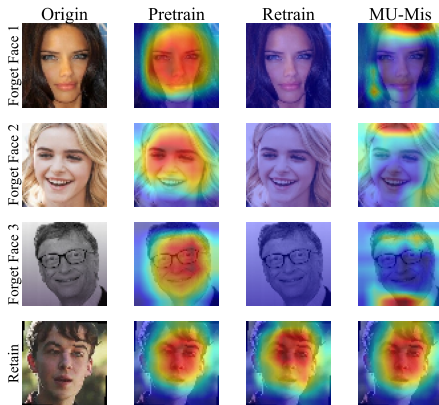
Method	No Jacob Regularization					Jacob Regularization = 0.01				
	FA	RA	TA	Avg. Gap↓	MIA	FA	RA	TA	Avg. Gap↓	MIA
Pretrain	88.54	83.59	84.03	32.54	0.9498	88.53	83.33	83.11	32.58	0.9436
Retrain	0.00±0.00	86.11±0.11	77.56±0.15	0.00	9.56±0.08	0.00±0.00	85.77±0.23	77.35±0.07	0.00	0.11±0.09
MU-Mis	1.40±0.35	84.13±0.28	75.98±0.52	1.62	0.98±0.12	5.67±0.32	82.37±0.14	75.12±0.07	3.77	0.21±0.09

1302  
1303 G.4 HYPER-PARAMETER SENSITIVITY  
1304

1305 We show that there is a clear relationship between the norm ratio and model performance during  
1306 unlearning in Figure A1. The stopping threshold ratio  $\delta$  controls the magnitude ratio of final irrelevant  
1307 class sensitivity norm  $\|\nabla_x f_{c'}(x, w)\|_F$  to initial one  $\|\nabla_x f_{c'}(x, w_p)\|_F$ . In this part, we investigate  
1308 the sensitivity of unlearning performance to  $\delta$  in Figure A2, taking fullclass-CIFAR100-Rocket with  
1309 ResNet-18 as an example. Different colors represent different  $\delta$ , ranging from 70% to 100%. The  
1310 green dashed line indicates the performance of the retrained model. Notably, under a specific learning  
1311 rate, the Avg. Gap exhibits minimal variation with changes in  $\delta$ . Generally, MU-Mis demonstrates  
1312 resilience against variations in hyper-parameters  $\delta$ . In summary, the hyper-parameter tuning for  
1313 MU-Mis is effortless, resilient and well-guided. This advantage in hyper-tuning indirectly enhances  
1314 the efficiency of unlearning and facilitates straightforward application of MU-Mis, making it valuable  
1315 for practical applications of MU methods.

1316  
1317 Figure A2: MU-Mis unlearning performance with different stopping threshold ratio under different  
1318 learning rates on fullclass-CIFAR100-rocket with ResNet-18. Performance varies little with the  
1319 threshold ratio when the learning rate is fixed.  
1320  
1321  
1322  
1323  
1324  
13251326 G.5 EFFECTIVENESS VISUALIZATION BY ATTENTION MAP  
1327

1328 To further investigate and understand the behavior  
1329 of our unlearned model, we showcase the attention  
1330 heatmaps (Selvaraju et al., 2017) of models before  
1331 and after applying MU-Mis on PinsFaceRecognition  
1332 dataset in Figure A3. For the forgetting data,  
1333 the original attention concentrates on the faces.  
1334 After applying MU-Mis, the attention on the faces  
1335 either disappears or significantly weakens, and is  
1336 shifted towards the background. For the remaining  
1337 data, MU-Mis fully maintains previous attention.  
1338 Notably, an alternative interpretation of input  
1339 sensitivity is the measurement of how changes in  
1340 the image influence its model prediction (Smilkov  
1341 et al., 2017). Our proposed method reduces the  
1342 target class logit sensitivity to the forgetting data  
1343 while recovering irrelevant classes', thereby en-  
1344 abling the unlearned model to disregard the seman-  
1345 tic information in the forgetting data meanwhile  
1346 preserve prediction sensitivity and performance  
1347 on the remaining data.  
1348  
1349

1350 Figure A3: **Visualization of attention maps**  
1351 for the full class unlearning task on PinsFace-  
1352 Recognition. MU-Mis distracts attention from  
1353 forgetting data regions while preserving atten-  
1354 tion on remaining data.

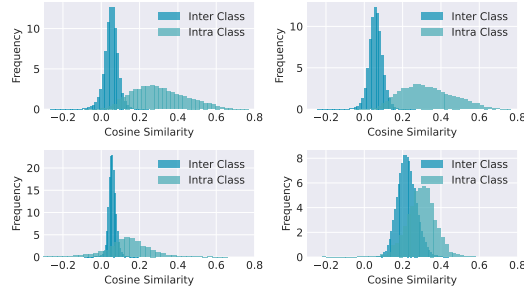
## 1350    H UNDERLYING REASONS FOR MODEL UTILITY PRESERVATION

1352    We suggest the favorable preservation on model utility might be attributed to two factors:

- 1354    • **Conceptual motivations:** The forgetting operation in MU-Mis differs fundamentally from  
1355    previous methods. While previous methods involved relabelling the forgetting data (Liu  
1356    et al., 2024; Foster et al., 2024a; Fan et al., 2024b) or knowledge distillation from a useless  
1357    teacher (Chundawat et al., 2023; Lin et al., 2023; Kurmanji et al., 2023), which unlearn by  
1358    introducing incorrect information to spoil original knowledge, MU-Mis unlearns by solely  
1359    withdrawing the contribution of forgetting data. In Figure A1, we show that RA and TA stay  
1360    at a high level throughout the withdrawal process.
- 1361    • **Empirical investigation:** Current gradient-based unlearning methods (Liu et al., 2024;  
1362    Foster et al., 2024a; Fan et al., 2024b; Wu et al., 2020; Graves et al., 2021; Neel et al.,  
1363    2021; Thudi et al., 2022) all employ cross-entropy loss gradient  $\nabla_{\theta}\mathcal{L}(w, x)$  to unlearn.  
1364    However, the intra-class gradients in a well-trained model are quite similar (Papyan, 2020;  
1365    Papyan et al., 2020). While the gradient of input sensitivity norm w.r.t parameters is double  
1366    back-propagation (Drucker & Le Cun, 1992), enhancing sample-specificity by first back-  
1367    propagating to the input samples before reaching the parameters. Our pairwise analysis  
1368    of cosine similarity among intra-class and inter-class samples, detailed in the following,  
1369    reveals a distinctive orthogonality in input sensitivity gradients, spontaneously reducing the  
1370    interference between the forgetting and remaining data.

1371    We calculate the pairwise cosine similarity within a class and between classes of the derivatives  
1372    of four metrics w.r.t. parameters in a well-trained model in Figure A4 to demonstrate an inherent  
1373    orthogonality input sensitivity view. They are  $\nabla_w\mathcal{L}$ ,  $\nabla_w f_c$ ,  $\nabla_w \|\nabla_x f_c\|_F$ , and  $\nabla_w \sum_{c' \neq c} \|\nabla_x f_{c'}\|_F$   
1374    (denoted as  $\nabla_w \|\nabla_x f_{c'}\|_F$  in the following for brevity). The first two metrics are commonly used  
1375    in current unlearning methods, and the last two are utilized in MU-Mis. Derivatives of all four  
1376    metrics are approximately orthogonal between samples from different classes. However, intra-class  
1377    similarities differ across four metrics. We can see that both  $\nabla_w\mathcal{L}$  and  $\nabla_w f_c$  bear a resemblance within  
1378    a class, with cosine similarity centering around 0.3 and reaching up to 0.6. While  $\nabla_w \|\nabla_x f_c\|_F$   
1379    centers around 0.1 with intra-class similarity scarcely exceeding 0.3. **Directly taking the derivative**  
1380    **of output w.r.t parameters preserves within-class similarity of the output, but such similarity is**  
1381    **reduced when output first takes the derivative to the input and then back to parameters.**

1381    Interestingly,  $\nabla_w \sum_{c' \neq c} \|\nabla_x f_{c'}\|_F$  seems to be pairwise similar. We speculate that there are two  
1382    reasons why this portion of our loss function does not significantly harm the performance of the  
1383    remaining data. Firstly, as shown in Figure 3,  $\sum_{c' \neq c} \|\nabla_x f_{c'}\|_F$  is significantly smaller than  $\|\nabla_x f_c\|_F$   
1384    on well-trained models. Therefore, in the early stages of optimizing the relative magnitudes of input  
1385    sensitivities, the contribution of  $\nabla_w \sum_{c' \neq c} \|\nabla_x f_{c'}\|_F$  to the optimization direction can be neglected.  
1386    Secondly,  $\sum_{c' \neq c} \|\nabla_x f_{c'}\|_F$  for the forgetting data actually corresponds to the target class of the  
1387    remaining data. The inter-class similarity of  $\nabla_w \sum_{c' \neq c} \|\nabla_x f_{c'}\|_F$  implies that when sensitivity of  
1388    other irrelevant classes increases, the input sensitivity of the remaining data of the corresponding  
1389    classes increases as well, thereby preserving their sample contributions.



1401    **Figure A4: Inter-class and intra-class cosine similarity of four different metrics w.r.t parameters.**  
1402    From left to right:  $\nabla_w\mathcal{L}$ ,  $\nabla_w f_c$ ,  $\nabla_w \|\nabla_x f_c\|_F$ , and  $\nabla_w \sum_{c' \neq c} \|\nabla_x f_{c'}\|_F$ . Directly taking the derivative of  
1403    output w.r.t parameters bears a resemblance across samples, but such similarity is reduced when  
1404    output first takes derivative to input and then back to parameters.

1404 **I DISCUSSION**  
 1405

1406 Beyond the advantages of input sensitivity for measuring sample contribution, we raise the attention  
 1407 that the input sensitivity perspective possesses a profound connection to MU. MU emerges from  
 1408 model’s memorization of the training data and seeks to safeguard the privacy of training data. Recent  
 1409 studies by Garg et al. (Garg et al., 2024) and Ravikumar et al. (Ravikumar et al., 2024) reveal the  
 1410 intrinsic relationship between memorization, privacy and sample’s input curvature. Also, Mo et al.  
 1411 (Mo et al., 2021) demonstrates that the input sensitivity of model gradient is the underlying cause of  
 1412 information leakage exposed by Model Inversion Attack (MIA) (Zhu et al., 2019; Zhao et al., 2020).  
 1413 Collectively, these works further underscore the inherent advantages of adopting an input sensitivity  
 1414 perspective for machine unlearning.

1415 **I.1 CORRELATIONS BETWEEN SENSTIVITY GAP AND LOSS CURVATURE IN FORMULA**  
 1416

1417 The loss curvature for memorization proxy used in Zhao et al. (2024); Zhao & Triantafillou (2024) is  
 1418  $\text{Curvature}(x) \propto \text{tr}(\nabla_x^2 \mathcal{L}(x))$ . For input sensitivity of loss, we have  
 1419

$$\begin{aligned} \nabla_x \mathcal{L}(x) &= (p - e_c)^\top \nabla_x f(x) = (1 - p_c) \nabla_x f_c(x) - \sum_{c' \neq c} p_{c'} \nabla_x f_{c'}(x) \\ &= \left( \sum_{c'=1}^C p_{c'} \right) \nabla_x f_c(x) - \sum_{c'=1}^C p_{c'} \nabla_x f_{c'}(x) = \sum_{c=1}^C p_c (\nabla_x f_c(x) - \nabla_x f_{c'}(x)). \end{aligned} \quad (\text{A5})$$

1420 By comparing the formula of loss curvature and sensitivity gap used in MU-Mis, we could see that:  
 1421

$$\text{tr}(\nabla_x^2 \mathcal{L}(x)) = \sum_{c=1}^C p_c \text{tr}(\nabla_x^2 (f_c(x) - f_{c'}(x))) \text{v.s.} \|\nabla_x f_c(x)\|_F^2 - \|\nabla_x f_{c'}(x)\|_F^2 \quad (\text{A6})$$

1422 While both terms reflects sensitivity gap between target class and irrelevant classes, they refers to  
 1423 different order of gradient. Specifically, **loss curvature** primarily aims at **second-order** sensitivity,  
 1424 while sensitivity gap in **MU-Mis** refers to the **first-order** sensitivity. Mathematically, it seems that  
 1425 there is no straightforward equality or conserved bound that could directly links this two metrics.  
 1426 Therefore, we’re afraid that we could not provide a general deterministic bound or functional  
 1427 equivalence without further assumptions.

1428 **I.2 INPUT SENSITIVITY SIGNATURES ACROSS DIFFERENT SAMPLES**  
 1429

1430 Although there is few clue of mathematical relationship for analysis, we further investigate their  
 1431 correlations by examining the sensitivity signatures across different samples empirically, *i.e.* samples  
 1432 of different memorization/influence levels.

1433 We partition training samples of CIFAR-10 dataset according to their sample-wise memorization  
 1434 score (provided by Feldman (2020); Feldman & Zhang (2020) through training many models on  
 1435 different held-out subsets to measure each sample’s self-influence on its own prediction) into low,  
 1436 middle, high memorization levels (following Zhao et al. (2024)). We partition training samples of  
 1437 CIFAR-100 dataset according to their influence score (provided by Feldman (2020); Feldman &  
 1438 Zhang (2020) through training many models on different held-out subsets to quantify each sample’s  
 1439 cross-influence on test data) into the same 3 levels. The scores are available at <https://github.com/google-research/heldout-influence-estimation..>

1440 Interestingly, the distributions of sensitivity gap of different sample groups are shown in Table A15. For  
 1441 memorization level, highly memorized samples exhibit smaller sensitivity gap than low and middle  
 1442 memorized sample. For influence score, more influencial samples exhibit higher sensitivity gap.  
 1443 Importantly, we think this empirical findings provide meaningful support for our use of sensitivity  
 1444 gap as a proxy for sample contribution.

1445 We evaluate MU-Mis when respectively unlearning samples with low, medium, and high memoriza-  
 1446 tion levels in Table A16. We could see that removing those highly-memorized samples causes a

1458 Table A15: Sensitivity gaps across memorization and influence levels on CIFAR-10 and CIFAR-100.  
1459

1460 1461 1462 1463 1464 1465 1466 1467 1468 1469 1470 1471 1472 1473 1474 1475 1476 1477 1478 1479 1480 1481 1482 1483 1484 1485 1486 1487 1488 1489 1490 1491 1492 1493 1494 1495 1496 1497 1498 1499 1500 1501 1502 1503 1504 1505 1506 1507 1508 1509 1510 1511	CIFAR-10 (Memorization Level)					CIFAR-100 (Influence Level)				
	Level	Mean	Std	10th	50th	90th	Mean	Std	10th	50th
Low	10.7632	4.2386	6.0814	10.0681	16.4851	36.1209	14.7241	19.3663	34.3506	56.0993
Mid	10.5156	5.5244	3.9959	10.0496	17.6092	39.3604	16.7700	21.3345	36.4983	61.0855
High	6.7922	6.0817	-0.7257	6.6459	14.5839	42.5803	17.1963	23.9295	39.5377	65.7531

more substantial utility drop in the remaining data, indicating that the performance of MU-Mis is not uniform across samples of different memorization levels. But maybe this is understandable, to some extent, expected, as unlearning highly entangled and influential samples is intrinsically difficult for any unlearning method Fan et al. (2024a); Zhao et al. (2024). We acknowledge this is an important limitation and a promising direction for future work, where more fine-grained unlearning mechanisms could be developed to further improve remaining-data-free unlearning.

Table A16: Performance of MU-Mis when unlearning low, middle, high levels of samples.

Memorization	Method	FA	RA	TA	Avg. Gap	MIA
Low	Original	100.00	100.00	85.10	0.45	0.013
	Retrain	99.83	100.00	83.93	0.00	0.049
	MU-Mis	100.00	99.96	83.32	0.27	0.041
Mid	Original	100.00	100.00	85.10	9.02	0.019
	Retrain	74.40	100.00	83.63	0.00	0.539
	MU-Mis	93.63	87.09	69.29	15.49	0.194
High	Original	100.00	100.00	85.10	26.83	0.055
	Retrain	21.63	100.00	82.99	0.00	0.811
	MU-Mis	46.10	66.79	57.03	27.88	0.607

### I.3 ESSENTIAL GOAL OF MU IN TERMS OF MEMORIZATION, GENERALIZATION AND SAMPLE CONTRIBUTION

There is an important question that might connect core idea of MU-Mis and RUM:

**Q1.** What's the correlation between sample contribution and memorization?

**Q2.** Is unlearning equivalent to alleviating sample's memorization level?

**Brief clarification between memorization, sample influence and sample contribution.**

1. **Memorization is defined as the change in its own prediction when a sample leaves the training set, i.e., self-influence.**
2. **Sample influence is the change on prediction of other data (test data), thereby more lies in cross-influence.**
3. **Sample contribution is the contribution of a training sample to all the model predictions, thereby comprising both the memorization (self-influence) and sample influence (cross-influence).**

**RQ1. Memorization level is not proportional to sample contribution.** On the one hand, high memorization can coincide with large contribution, *e.g.*, long-tail but but genuinely informative examples, the model may need to “memorize” them to support generalization. On the other hand, high memorization does not guarantee substantial contribution: a model might over-fit noise, duplicates, or outliers, thereby exhibiting strong memory for those examples even though they contribute little or may harm the remaining data’s performance. Conversely, a training example may exert substantial influence on the model’s remaining predictions (high contribution) without having been deeply memorized (low memorization).

**RQ2. Minimizing sample contribution is more essential for unlearning than reducing memorization.** Generally, in random subset case, to unlearn an instance, we would aim to alleviate model’s memorization of it to prevent privacy leakage exploited by MIA. However, as discussed above, memorization (self-influence) and influence (cross-influence) consist sample contribution

1512 together. Therefore, in a broader sense, de-memorization is not that enough for a complete removal,  
1513 while withdrawing sample contribution is more fundamental.

1514  
1515 In light of the effectiveness of MU-Mis in full/sub-class unlearning, where removal is beyond merely  
1516 reducing memorization, we think MU-Mis is not limited to directly alleviate memorization by  
1517 optimizing certain curvature-based measures. Rather, we prefer to view MU-Mis as a practical and  
1518 efficient proxy that could implicitly reduce memorization by suppressing a sample’s contribution.  
1519 Additionally, given the less satisfactory results of MU-Mis in the random-subset unlearning setting,  
1520 we suspect that a direct optimization of loss curvature (*i.e.*, explicitly minimizing loss curvature  
1521 around a specific sample) might be sufficient to prevent privacy leakage and yield better model-utility  
1522 trade-offs in this scenario.

1522

1523

## J LIMITATION

1524

1525 Although MU-Mis could achieve comparable performance to SoTA remaining-data-dependent meth-  
1526 ods, there is a clear room for further improvement in the most challenging unlearning scenario,  
1527 random subset unlearning. We fully acknowledge that our investigation is quite preliminary, but  
1528 we believe that the input sensitivity might be a valuable and beneficial perspective for developing  
1529 remaining-data-free unlearning, which is collectively demonstrated by MU-Mis and RUM, leaving a  
1530 good starting point for future study.

1531

1532

1533

1534

1535

1536

1537

1538

1539

1540

1541

1542

1543

1544

1545

1546

1547

1548

1549

1550

1551

1552

1553

1554

1555

1556

1557

1558

1559

1560

1561

1562

1563

1564

1565